Two qubit gates for Gottesmann-Kitaev-Preskill states

and their implementations

Paul Moser Röggla
paulmo@student.ethz.ch

Supervisors:
Dr. Florentin Reiter
Ivan Rojkov
Martin Wagener
Prof. Jonathan Home

A thesis presented for the degree of
Master of Science

Trapped Ion Quantum Information Group
ETH Zürich
April 8, 2022

Abstract

Two qubit gates are essential for universal quantum computation. For Gottesmann-Kitaev and Preskill states, two qubit gates like the CZ and the CNOT can be realized using optical elements such as squeezers and beamsplitters. They are designed however for idealized GKP codewords, therefore finite energy effects arise in a realistic setting. In this thesis we will give ways to quantify those finite energy effects in GKP states in phase space. We will calculate explicitly the change of the wave function for a computational basis state before and after the application of the logical CZ. We observe for the CZ gate, that in phase space all errors occur in the p quadrature, whereas the q quadrature stays untouched. A full understanding of the errors induced by the CZ gate would allow to design precise error correction schemes to correct for the errors. We give a novel approximate scheme of the GKP CZ gate and compare it to existing schemes for the GKP CNOT gate. We finally will look at error correction schemes that correct the finite energy effects.

Acknowledgements

I would like to thank Dr. Florentin Reiter for his excellent supervision throughout the time working on my thesis and Prof. Jonathan Home to give me the possibility to perform my Master's Thesis within the TIQI group.
I would like to thank Ivan Rojkov for his inputs and help on a daily basis for my Thesis. He helped with my physical understanding as well as my problems concerning numerics and analytics.
I would like to furthermore thank Martin Wagener and Moritz Fontbotè Schmidt for our weekly meetings, which gave me the opportunity to get an insight into the more experimental work on GKP qubits and their helpful inputs throughout my work.

Contents

Chapter 1

Introduction to GKP states

1.1 Introduction

Quantum computation could represent a possible paradigm shift in Computational science as quantum algorithms are favourable candidates to outplay their classical counterpart as seen for example in Grover's- [12] or Shor's period finding algorithm [22]. Realizable universal quantum computation (UQC) however has been a big challenge, since the introduction of quantum computers in the 1980s [7]. Realizability requires that quantum computation should both be technically implementable and robust against errors. One approach to achieve robustness to errors is to encode one logical qubit into multiple physical qubits. Then error detecting measurements on the physical qubits can be used to determine whether an error occurred. Such an encoding effectively enhances the dimension of the Hilbert space. A state-of-the-art example for this is the Shor code [23]. Encoding logical qubits into multiple physical qubits can become very costly, since only few physical qubits can thus far be implemented in an experimental setting (see for example the work in reference [1]).
Continuous variable quantum computation takes a different approach. The dimension of the Hilbert space of a harmonic oscillator is infinite. Errors then occur in the form of phase space displacements. This is the starting point for the so called Gottesmann-Kitaev-Preskill qubits [11], where information is stored in the phase space of a harmonic oscillator. In order to obtain UQC we need to be able to perform single qubit and two qubit gates such as the CNOT or the CZ gate . The latter will be the main interest of this thesis.
In this chapter we will introduce the quantum harmonic oscillator in phase space, the structure of a quantum computational code and we will introduce the ideal and finite energy GKP states.

1.1.1 Quantum harmonic oscillator and phase space

The quantum harmonic oscillator is described via the Hamiltonian

$$H = \frac{p^2}{2} + \frac{1}{2}q^2, \tag{1.1}$$

where p is the momentum operator and q is the position operator. We assumed $\hbar = 1$. Systems such as photons and the trapped ions' motion can be described via this Hamiltonian. It describes the quantum mechanical analogue to a system with harmonic oscillations. The allowed energies of a harmonic oscillator are described by the time independent Schrödinger equation

$$H\left|\psi\right\rangle = E\left|\psi\right\rangle, \tag{1.2}$$

where $\left|\psi\right\rangle$ is a quantum state and E is an energy eigenvalue. By introducing the ladder operators

$$a = \frac{1}{\sqrt{2}}(q+ip) \qquad \text{and} \qquad a^\dagger = \frac{1}{\sqrt{2}}(q-ip), \tag{1.3}$$

the Hamiltonian can be rewritten as

$$H = n + \frac{1}{2}, \tag{1.4}$$

where we defined the number operator $n = a^\dagger a$, which acting on a energy eigenstate $|n\rangle$ returns the number of energy quanta n. The lowest achievable energy state is called the ground state.
By solving directly equation (1.2), you can obtain the eigenfunctions of the Hamiltonian, which are given by

$$\psi(q) \propto e^{-\frac{q^2}{2}} H_n(q), \tag{1.5}$$

where $H_n(z) = (-1)^n e^{\frac{z^2}{2}} \partial_z^n (e^{-\frac{z^2}{2}})$ are the Hermitian polynomials. By setting $n = 0$ we can obtain the ground state explicitly in position space to find

$$|g\rangle \propto \int dq e^{-\frac{q^2}{2}} |q\rangle, \tag{1.6}$$

where the integral goes over all eigenstates of the position operator. This means that the ground state in position space is proportional to a Gaussian with unit variance.
Position space has a reciprocal space, which is the momentum space. The combination of the two is called phase space. The q and p variable are often referred to as the quadratures of the phase space. The momentum space representation of the wave function can be obtained by Fourier transforming the position wave function. In terms of states this can be obtained by a basis change as shown in equation (1.7)

$$\int dq\psi(q) |q\rangle = \mathbb{1} \int dq\psi(q) |q\rangle = \int dp \int dq\psi(q) \langle p|q\rangle |p\rangle = \int dp\mathcal{F}[\psi(q)] |p\rangle, \tag{1.7}$$

where $\mathcal{F}[\cdot]$ is the Fourier Transform and we used the following representation of the identity:

$$\mathbb{1} = \int dp |p\rangle \langle p| = \int dq |q\rangle \langle q|. \tag{1.8}$$

When moving between the spaces the following relations between position and momentum basis states are important:

$$\langle x|q\rangle = \delta(q - x), \qquad \langle p|q\rangle = e^{-ipq} \qquad \text{and} \qquad \int dq\delta(q - x)f(q) = f(x), \tag{1.9}$$

where $|q/p\rangle$ mark a position and momentum eigenstate respectively.
In this thesis we work mostly in phase space. For more details on the quantum harmonic oscillator we refer the reader to any introductory textbook on quantum mechanics.

1.1.2 Crash course on quantum computation

The most elemental blocks of quantum computation are qubits. Qubits are manipulated via unitary operations, which are called gates. Consider a two level system. The state of a qubit is then described via a superposition of computational basis states, which is given by

$$|\psi\rangle = \cos\left(\frac{\theta}{2}\right) |0\rangle + e^{i\alpha} \sin\left(\frac{\theta}{2}\right) |1\rangle. \tag{1.10}$$

The computational basis states are eigenstates of the logical Z operator, which has the properties

$$Z|0\rangle = |0\rangle \qquad \text{and} \qquad Z|1\rangle = -|1\rangle. \tag{1.11}$$

By performing a basis change via the so called Hadamard gate H on the computational basis states you obtain the $|\pm\rangle$ basis. The $|\pm\rangle$ states are eigenstates to the logical X operator in the same way as the $|0/1\rangle$ states for the Z operator. It is possible to store the information of a single logical qubit in multiple physical qubits. If you consider for instance n physical qubits, you can write your logical basis states as $|0\rangle_L = |\psi_1\rangle \otimes ... \otimes |\psi_n\rangle$ and $|1\rangle_L = |\phi_1\rangle \otimes ... \otimes |\phi_n\rangle$. The logical basis states are the so called codewords, and the codewords span the logical subspace known as code space.
If you can perform any unitary operation to n qubits you enabled universal quantum computation (UQC). In order to obtain UQC you must be able to perform four distinct gates, which form a universal set of gates (this set is not unique). These gates are

$$Univ = (H, S, CNOT, T). \tag{1.12}$$

The Hadamard gate is the basis changing gate from before, the S gate is a phase gate which acts as $S|0\rangle = |0\rangle$ and $S|1\rangle = i|1\rangle$. It is connected to the logical Z operator via $S^2 = Z$. The T gate introduces a different phase and acts as $T|0\rangle = |0\rangle$ and $T|1\rangle = e^{i\frac{\pi}{4}}|1\rangle$. The CNOT gate is a two qubit gate, which acts on the second qubit conditioned on the state of the first qubit. The CNOT is given by

$$CNOT = |0\rangle\langle 0| \otimes I + |1\rangle\langle 1| \otimes X. \tag{1.13}$$

It performs a logical X operator on the target qubit, if the control qubit is in $|1\rangle$. The two qubit gate does not have to be the CNOT. Another valid choice is the CZ gate. The CZ is obtained by performing a basis change via the H gate on the target qubit. The CZ performs a logical Z gate on the target, if the control qubit is in state $|1\rangle$. It is given by:

$$CZ = |0\rangle\langle 0| \otimes I + |1\rangle\langle 1| \otimes Z. \tag{1.14}$$

The H, S and $CNOT$ generate the so-called Clifford group. For a more detailed introduction of quantum computation, refer to [18].
An important concept in quantum error correction is the notion of a stabilizer. A stabilized state by an operator K is a state for which

$$K|\psi\rangle = |\psi\rangle. \tag{1.15}$$

In quantum computation the codewords are stabilized by a proper set of stabilizers. For a more detailed analysis of stabilizers refer to the thesis of D. Gottesman [9].

1.1.3 Gottesmann-Kitaev-Preskill qubits

GKP qubits have been first introduced by Gottesmann Kitaev and Preskill [11]. The main idea is to store information in the phase space of a harmonic oscillator. We will often refer to the GKP states either as GKP qubits or continuous variable modes. Gates are then applied by either displacing, squeezing or rotating the states. We distinguish between ideal and finite energy GKP states. Assume therefore from now on, unless stated otherwise, that our qubits are laid out on a rectangular grid, where one direction marks the position and the perpendicular direction marks the momentum direction.

Ideal GKP qubits

As a first step when talking about quantum computation we should introduce computational basis states, the logical operators, the commutation relations between the logical operators and stabilizers. As mentioned before, we are laying out our information on a phase space grid with even spacing. This means that we have a translational symmetry that we can exploit. Assume that our grid points are separated by a spacing of $\sqrt{\pi}$. The logical operators are defined as displacements along the position or the momentum axis. Let q and p be the position and momentum operator and q, p their respective eigenvalues. The logical operators are then defined as

$$\mathrm{Z}_L = \exp\left(i\sqrt{\pi}q\right) \tag{1.16}$$
$$\mathrm{X}_L = \exp\left(-i\sqrt{\pi}p\right), \tag{1.17}$$

and our logical states are an infinite superposition of position and momentum eigenstates:

$$|0\rangle_L = \sum_{j=-\infty}^{\infty} |q = \sqrt{\pi}2j\rangle \text{ and } |1\rangle_L = \sum_{j=-\infty}^{\infty} |q = \sqrt{\pi}(2j+1)\rangle \tag{1.18}$$
$$|+\rangle_L = \sum_{j=-\infty}^{\infty} |p = \sqrt{\pi}2j\rangle \text{ and } |-\rangle_L = \sum_{j=-\infty}^{\infty} |p = \sqrt{\pi}(2j+1)\rangle. \tag{1.19}$$
$$\tag{1.20}$$

Note that the subscript L refer to the logical subspace, whereas states without subscript to physical states. We will later on drop the subscript L for better readability.The computational basis states are shown in Figure 1. It can be seen that the $|0/1\rangle_L$ states are eigenstates to the logical operator Z_L and $|\pm\rangle_L$ are

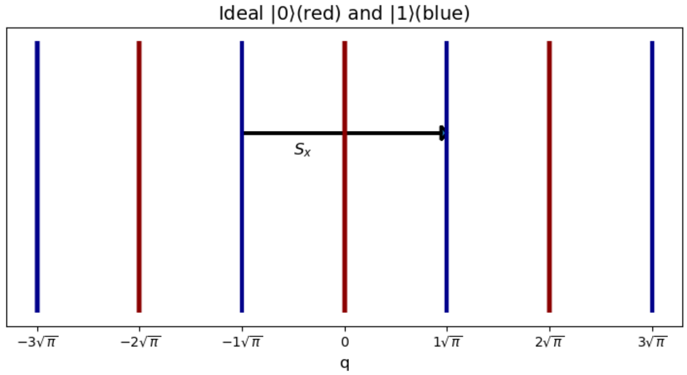

Figure 1.1: Ideal computational basis states. We can see that the logical $|0\rangle$ is a superposition of position eigenstates spaced by even multiples of $\sqrt{\pi}$. The logical $|1\rangle$ state is constructed similarly, with the eigenstates being spaced by odd multiples of π. We can also see the translational invariance under application of the stabilizers.

eigenstates to X_L. This follows by expanding the operator into its Taylor series form and applying the individual operators to a position or momentum eigenstate respectively:

$$Z_L |q\rangle = e^{i\sqrt{\pi}q} |q\rangle = \sum_n \frac{(i\sqrt{\pi}q)^n}{n!} |q\rangle = e^{i\sqrt{\pi}q} |q\rangle \tag{1.21}$$

$$X_L |p\rangle = e^{-i\sqrt{\pi}p} |p\rangle = \sum_n \frac{(-i\sqrt{\pi}p)^n}{n!} |p\rangle = e^{-i\sqrt{\pi}p} |p\rangle . \tag{1.22}$$

We can see that that the logical operators show the desired behaviour by noting that the X_L operator shifts the position operator by $\sqrt{\pi}$ and similarly for the Z_L operator with the momentum operator. This means that the X_L performs a bit flip on the $|0/1\rangle_L$ state and Z_L introduces a phase as desired. In the equations above we used, that the states of interest are eigenstates of the exponent of the respective operator. As mentioned before we finally must introduce the commutation relations between the logical operators. We want that the commutation relations match their discrete variable counterparts

$$[\sigma_a, \sigma_b] = 2i\varepsilon_{abc}\sigma_c, \tag{1.23}$$

with ε being the Levi Civita tensor and σ_i the different Pauli matrices. We have seen that in the GKP setting the logical operators are displacements in phase space. The general definition of a displacement in phase space by a complex number α is given by

$$D(\alpha) = \exp\left(i\sqrt{2}(\mathrm{Im}(\alpha)q - \mathrm{Re}(\alpha)p)\right). \tag{1.24}$$

Two displacements generally do not commute but obey the following commutation rule

$$D(\alpha)D(\beta) = e^{i(\mathrm{Im}(\alpha\beta^*))}D(\beta)D(\alpha). \tag{1.25}$$

With this knowledge, we can write our logical operators in terms of a general displacement $D(\alpha)$ and calculate the commutation relations. We have

$$X_L = D\left(\sqrt{\frac{\pi}{2}}\right) \text{ and } Z_L = D\left(i\sqrt{\frac{\pi}{2}}\right), \tag{1.26}$$

for our logical operators and therefore by using equation (1.25):

$$[X_L, Z_L] = e^{-i\frac{\pi}{2}} D\left((i+1)\sqrt{\frac{\pi}{2}}\right) \propto iY_L. \tag{1.27}$$

This exhibits the same behaviour as equation (1.23).
The codewords are invariant under translations of $2\sqrt{\pi}$ along q for $|0\rangle, |1\rangle$ and invariant under translations

of $2\sqrt{\pi}$ along p for $|\pm\rangle$. We define the stabilizers as displacements of $2\sqrt{\pi}$ in their respective direction. These are given by:

$$S_z = e^{i2\sqrt{\pi}q} \text{ and } S_x = e^{-i2\sqrt{\pi}p}. \tag{1.28}$$

This gives a full description of the GKP code. The ideal computational basis states are however non normalizable. This can be seen since every term in the sums in equations (1.18) consists of δ peak. The δ peaks can be obtained explicitly if we project explicitly the position eigenstates into position space and the momentum eigenstates into momentum space. For example for the logical 0 state we obtain:

$$\psi_{|0\rangle}(q) = \langle q|0\rangle = \sum_{s\in\mathbb{Z}} \delta(q - 2s\sqrt{\pi}). \tag{1.29}$$

To see that this is indeed non-normalizable it is sufficient to look at a single δ function $\delta(q-a)$. The Fourier transform of a δ peak is given as

$$\int dq e^{-ipq}\delta(q-a) = e^{-iap}. \tag{1.30}$$

Normalizability requires

$$\int dp|\psi(p)|^2 = 1. \tag{1.31}$$

Setting $\psi(p) = e^{-iap}$ and using $|e^{-iap}| = 1$, we see that the normalizability for a δ function is not fulfilled. To fix this issue, we define realizable, finite energy GKP qubits in the next section.

Finite Energy GKP Qubits

The ideal GKP states can either be seen as a sum of δ peaks, or as a sum of infinitely squeezed displaced vacuum states. Squeezing is a unitary operation used to enhance the resolution in one quadrature in phase space, while reducing the resolution in the other quadrature. The unitary operator in phase space associated to the squeezing operator is

$$S(r) = \exp\big(\frac{r}{2}(qp + pq)\big). \tag{1.32}$$

In this thesis we will consider two different types of squeezing parameters, r and Δ. They are connected via the following relation:

$$r = -\log\Delta, \tag{1.33}$$

with log being the natural logarithm. We will encounter squeezing in two different scenarios: In the state preparation, as we will describe below, and in the manipulation of GKP gates, as will be discussed in chapter 4. To avoid confusion between the parameters, we will use the parameter Δ for state preparation and the parameter r for implementations of gates in chapter 4.

The squeezing operator applied to the ground state gives a squeezed state and is given by:

$$S(-\log(\Delta))\,|g\rangle \propto \int_{-\infty}^{\infty} \frac{dq}{(\pi\Delta^2)^{\frac{1}{4}}} e^{-\frac{q^2}{2\Delta^2}}\,|q\rangle\,, \tag{1.34}$$

where the ground state is defined as in equation (1.6).

For our computational basis states we require the states to be displaced along either the q or p axis. A squeezed state, displaced by an amount a along the q axis is given by

$$D(\frac{ia}{\sqrt{2}})S(-\log(\Delta))\,|g\rangle \propto \int_{-\infty}^{\infty} \frac{dq}{(\pi\Delta^2)^{\frac{1}{4}}} e^{-\frac{(q-a)^2}{2\Delta^2}}\,|q\rangle\,. \tag{1.35}$$

The ideal logical $|0\rangle$ can therefore be written as

$$|0\rangle = \lim_{\Delta\to 0} \sum_{j=-\infty}^{\infty} D\bigg(\frac{i(2s\sqrt{\pi})}{\sqrt{2}}\bigg) S(-\log(\Delta))\,|g\rangle\,. \tag{1.36}$$

We require this to be normalizable. Therefore we assume that $\Delta > 0$, which replaces every infinitely squeezed state by a finitely squeezed state. Finally to obtain a normalizable wave function we multiply the superposition of displaced squeezed states with a Gaussian envelope of width κ^{-1}. We obtain the following result

$$|0\rangle_{\text{finite}} = \mathcal{N}_0 \sum_{s\in\mathcal{Z}} e^{-\frac{1}{2}\kappa^2(2s\sqrt{\pi})^2} \int \frac{dq}{(\pi\Delta^2)^{\frac{1}{4}}} e^{-\frac{(q-2s\sqrt{\pi})^2}{2\Delta^2}} |q\rangle \tag{1.37}$$

$$|1\rangle_{\text{finite}} = \mathcal{N}_1 \sum_{s\in\mathcal{Z}} e^{-\frac{1}{2}\kappa^2((2s+1)\sqrt{\pi})^2} \int \frac{dq}{(\pi\Delta^2)^{\frac{1}{4}}} e^{-\frac{(q-(2s+1)\sqrt{\pi})^2}{2\Delta^2}} |q\rangle \,. \tag{1.38}$$

These are the same form as reported in the original GKP paper [11]. The Wigner functions which is going to be introduced in chapter 2, of the computational basis states are shown in Figure 2. We can

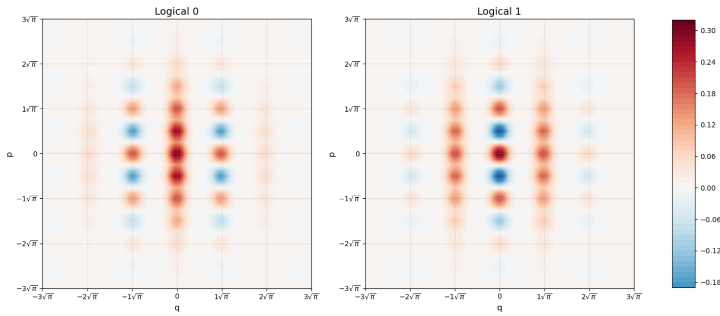

Figure 1.2: Wigner quasi-probability function of finite energy $|0\rangle, |1\rangle$

see that for the logical 0 peaks occur at even multiples of $\sqrt{\pi}$ whereas for the logical 1 we can observe a similar behaviour for odd multiples of $\sqrt{\pi}$. For the ideal GKP states this grid would be infinite in both directions, whereas in the plot above the finite Gaussian envelope appears. This can be seen from the decrease of the peaks' contrast as $q \to \pm\infty$ and $p \to \pm\infty$.
This is not the only possible way to introduce a finite energy GKP state. Another approach, which is taken in Mensen [16] defines the finite energy GKP states using the Jacobi theta function. The theta function, needed to define the Jacobi theta function is given by

$$\theta \begin{pmatrix} v_1 \\ v_2 \end{pmatrix} (z, \tau) = \sum_{n\in\mathbb{Z}} e^{2\pi i(\frac{1}{2}(n+v_1)^2\tau + (n+v_1)(z+v_2)}, \tag{1.39}$$

where $\text{Im}(\tau) > 0$ and $z \in \mathbb{C}$ and $v_1, v_2 \in \mathbb{Q}$. This function can be extended to a T periodic function, namely the Jacobi theta function, which is given by:

$$\theta_T \begin{pmatrix} v_1 \\ v_2 \end{pmatrix} (z, \tau) = \frac{1}{\sqrt{|T|}} \theta \begin{pmatrix} v_1 \\ v_2 \end{pmatrix} \left(\frac{z}{T}, \frac{\tau}{T^2}\right). \tag{1.40}$$

This function is structurally similar to what we obtained above for the finite energy GKP state as the summation in both terms contains linear and quadratic terms in the exponent for the summation variable. In fact, when considering the set of parameters, where $z = q$, $\tau = 2i\pi\Delta^2$, $v_1 = j/2$ and $v_2 = k/2$, where $j = k = 0/1$ this gives Gaussians displaced along q. If for instance $j = k = 0$ we apply Gaussians at every multiple of π with width Δ^2. For a finite energy GKP state we also require a Gaussian envelope. The envelope is obtained, by applying a non unitary error operator to the state

$$|\psi\rangle \propto \int dq \theta_{2\sqrt{\pi}} \begin{pmatrix} 0 \\ j/2 \end{pmatrix} (x, 2\pi i\Delta^2) |q\rangle \,. \tag{1.41}$$

The non unitary error operator is given by

$$\xi(\Xi) \approx R^\dagger(\phi) e^{-\frac{1}{2}\kappa^2 q^2} e^{-\frac{1}{2}\Delta^2 p^2} R(\phi), \tag{1.42}$$

where $R(\phi)$ is a rotation matrix. The first exponential in the state above applies an envelope to the state in position space with variance κ^{-2}, as can be seen by

$$e^{-\frac{1}{2}\kappa^2 q^2} |\psi\rangle \propto \int dq e^{-\frac{1}{2}\kappa^2 q^2} \psi(q) |q\rangle \,. \tag{1.43}$$

A similar calculation in p shows the application of an envelope with width Δ^{-2}. Multiplying the envelope with the Jacobi theta function we obtain the following formula for the wave function of a finite energy GKP state:

$$\psi_j(x) = \sqrt{\frac{4\pi\Delta}{\kappa}} G_{\kappa^{-2}}(x)\theta_{2\sqrt{\pi}} \begin{pmatrix} 0 \\ j/2 \end{pmatrix} (x, 2\pi i \Delta^2). \tag{1.44}$$

For $j = 0$ we obtain the logical 0 and for $j = 1$ we obtain the logical 1. This description is completely equivalent to the one above, as has been proven in [15].

While this allows for a finite energy description of our states, we still have the problem that our logical operations are designed to work for ideal GKP states.A common solution is to introduce finite energy versions of logical gates. This requires the so called finite energy operator as for example given in Tzitrin et al [25]. This operator is given by

$$E(\varepsilon) = \exp(-\varepsilon n), \tag{1.45}$$

where n is the number operator $n = \frac{1}{2}(q^2 + p^2)$ and ε is the damping factor. Note that this operator is non-unitary. This can be seen as

$$E(\varepsilon)^\dagger = \left(e^{-\varepsilon n}\right)^\dagger = \left(e^{-\varepsilon n}\right) \neq E(\varepsilon)^{-1} \tag{1.46}$$

To obtain the finite energy version of a gate we have to conjugate the ideal gate with the finite energy operator. This induces the following transformation for a gate U

$$U_I \rightarrow E(\varepsilon) U E(-\varepsilon) = U_\varepsilon \tag{1.47}$$

A finite energy gate acting on a finite energy state can now be written as:

$$U_\varepsilon \left|\psi_\varepsilon\right\rangle = E(\varepsilon) U_I E(-\varepsilon) E(\varepsilon) \left|\psi_I\right\rangle = E(\varepsilon) U_I \left|\psi_I\right\rangle, \tag{1.48}$$

where the subscript ε stands for the finite energy versions, whereas the subscript I stands for the ideal versions. It follows that a finite energy operator operating on a finite energy state can be seen as an ideal operator acting on an ideal state, which then is turned into a finite energy version. While in principle this sounds desirable there is still the issue of the non-unitarity. We will therefore later on discuss the arising errors when an ideal GKP gate acts on a finite energy GKP state.

The finite energy GKP states are no longer ideal $+1$ eigenstates of the stabilizer operators, defined in the previous chapter. Similarly, the logical operators are also only approximate and not ideal any more. The computational basis states are also not completely orthogonal. It can however be shown [11] that for a proper choice of Δ and κ the overlap of the computational basis states can be sufficiently suppressed.

Since the main goal of this thesis is to understand the mechanism of two qubit continuous variable gates we now proceed to introduce Gaussian quantum information as well as the group structures of the Heisenberg Weyl- and the symplectic group. These are necessary mathematical tools in order to properly introduce two qubit gates for GKP states.

Chapter 2

Theoretical background on two qubit GKP gates

2.1 Gaussian quantum information

2.1.1 Bosonic systems

We are working with bosonic systems. The Hilbert space of a bosonic system is given by the Fock space

$$\mathcal{H} = \bigoplus_{N=0}^{\infty} \mathcal{S}\mathcal{H}^{\otimes N}, \tag{2.1}$$

where $\mathcal{S}$ is the symmetrizing operator. If we are only interested in the first N particles this reduces to a correctly symmetrized tensor product of N Hilbert spaces. Bosons obey the Bose statistics and have a symmetric wave function. This translates in second quantization to creators and annihilators, which have commutation relations. Concretely, the bosons define the algebra

$$[a_k, a_j^\dagger] = \delta_{kj}, \qquad [a_k^\dagger, a_j^\dagger] = 0, \qquad [a_k, a_j] = 0 \tag{2.2}$$

Recalling the relations of the phase space variables for the quantum harmonic oscillator we find

$$q = \frac{1}{\sqrt{2}}(a^\dagger + a) \qquad \text{and} \qquad p = \frac{i}{\sqrt{2}}(a^\dagger - a), \tag{2.3}$$

for the position and momentum operator. Written in vector notation $x_i = (q_i, p_i)$, we find the symplectic form

$$[x_i, x_j] = \Omega_{ij} \tag{2.4}$$

where Ω_{ij} is the generic element of the symplectic form. The symplectic form is given by

$$\Omega = \bigoplus_i \omega_i = \begin{pmatrix} \omega & 0 & \cdots & 0 \\ 0 & \omega & 0 & \cdots \\ \vdots & \vdots & \ddots & \ddots \\ 0 & & \cdots & \omega \end{pmatrix}, \tag{2.5}$$

where $\omega = \begin{pmatrix} 0 & -1 \\ 1 & 0 \end{pmatrix}$. Hence Ω is a $2N \times 2N$ matrix. A matrix is said to be symplectic if

$$M^T \Omega M = \Omega \tag{2.6}$$

The symplectic group will be discussed in more detail in section 2.2.2. In a bosonic system the symplectic form arises due to the commutation relations in equation (2.2).

2.1.2 From density matrices to phase space representations

A quantum state can be fully described by its density operator ρ. The density operator is a non-negative operator with unit trace given by

$$\rho = \sum_i p_i \left|\psi_i\right\rangle \left\langle\psi_i\right|, \tag{2.7}$$

where p_i marks the probability to find the system in $|\psi_i\rangle$ when measured in a specific basis. A state is considered pure if its density matrix corresponds to a projector, hence

$$\rho = \left|\psi\right\rangle \left\langle\psi\right|. \tag{2.8}$$

Otherwise it is called a mixed state. A completely mixed state is given if the density operator corresponds to a multiple of the identity operator. The density operator allows for a full description of a quantum mechanical system. It is however not the only description of a quantum state. An equivalent description is given by the Wigner function in phase space. The derivation follows closely the one given in the Gaussian quantum information paper by Weedbrook et al [26]. First we define the Weyl operators and the characteristic function as

$$D(\xi) = \exp\left(ix^T\Omega\xi\right) \tag{2.9}$$

$$\chi(\xi) = \mathrm{Tr}(\rho D(\xi)), \tag{2.10}$$

where $\xi \in \mathbb{R}^{2n}$ and $x = (q_1, p_1, .., q_n, p_n)$ is a vector containing all the phase space operators.
The Wigner function is then the Fourier transform of the characteristic function and therefore given by

$$W(x) = \int_{R^{2n}} \frac{d^{2n}\xi}{(2\pi)^{2n}} \exp\left(-ix^T\Omega\xi\right)\chi(\xi) \tag{2.11}$$

The Wigner function is a quasi-probability distribution, meaning it is normalized, real and can assume both positive and negative values. Note that in the definition of the Wigner function in the exponent we do not have an operator but we have the eigenvalues of the quadrature operators. These span out the whole phase space. This means that a n mode density matrix and its $n \times n$ Wigner function in Phase space give an equivalent description. The modulus squared of the wave functions in the q/p quadratures can be obtained by marginalizing out the Wigner function. Wigner functions are a useful tool to display GKP qubits in phase space. They have an additional role, namely they allow us to characterize our state into Gaussian and non Gaussian states from the form of the Wigner function. A state is said to be Gaussian if its Wigner function has a Gaussian shape and is bosonic. This can be extended to Gaussian operations and Gaussian channels: An operation is Gaussian if it maps Gaussian states onto Gaussian states. These are unitaries which are quadratic in the quadrature operators (or in the annihilation and creation operators respectively). Gaussian operation can in phase space be characterized by the following relation:

$$(S, d) : x \to S \cdot x + d, \tag{2.12}$$

where x is a vector containing all quadrature operators and S is a symplectic matrix and d is a displacement. To fully characterize a Gaussian operation we finally need to know how the covariance matrix of the quadrature operators changes. This change is obtained by the following relation:

$$V \to S^T V S. \tag{2.13}$$

GKP states are not Gaussian, since as we have seen they have negative parts in the Wigner function (this can be seen in Figure 2). However in the work of Bourassa et al [5] it can be shown that the discussion of a Gaussian Wigner function can be extended to a linear superposition of Gaussian Wigner functions. We can therefore use the knowledge from Gaussian states and extend it to GKP states.
With the knowledge of symplecticity in Phase space, Gaussian quantum information and the logical structure of a GKP Qubit we can now look at gates and UQC in the context of GKP qubits.

2.2 GKP gates and Universal Quantum Computation

We introduced two single mode GKP gates at the very beginning of this thesis, the logical Z_L and the logical X_L which were displacements along the q, p axis respectively. We will now look into the more general group-structure of the displacements.

2.2.1 Heisenberg Weyl group

We will follow the structure from the paper of Peremolov [19] and the thesis from Weigand [8]. Let us remind ourselves of the general form of a displacement in terms of the quadrature operators

$$D(\alpha) = \exp\left(i\sqrt{2}(\mathrm{Im}(\alpha)q - \mathrm{Re}(\alpha)p)\right).$$

These are elements of the so called Heisenberg Weyl group. The Lie algebra of the Weyl Heisenberg group is determined by the bosonic commutation relations from equation (32)-(36). The most general form of an element of the Heisenberg Weyl group is then obtained via the exponential map between Lie algebra and Lie group and is given by the translation

$$T(t, \alpha) = e^{it} D(\alpha), \tag{2.14}$$

where t is a real parameter. If such an operator $T(t, \alpha)$ acts on the vacuum state we obtain a coherent state, i.e.

$$T(t, \alpha) |0\rangle = e^{it} D(\alpha) |0\rangle . \tag{2.15}$$

A GKP state is a superposition of displaced coherent states times a Gaussian envelope, and the logical GKP operators fall into this group. We will often write a displacement along the q axis with $T(a) = D(i\frac{a}{\sqrt{2}})$, this is not to be confused with the T operator given above, which depends on two parameters.

2.2.2 Symplectic group $Sp(2n, \mathbb{R})$

In Gaussian quantum information an additional symmetry group appeared, the symplectic group. The symplectic group $Sp(2n, \mathbb{R})$ is defined as

$$Sp(2n, \mathbb{R}) = \{M \in \mathrm{Mat}_{2n\times 2n}(\mathbb{R}) | M^T \Omega M = \Omega\}, \tag{2.16}$$

where Ω is the symplectic form as defined before in equation (2.5). All the matrices that leave invariant the symplectic form fall into this group. Since we are looking at transformations in phase space, the matrices are of dimension $2n \times 2n$. As already previously shown this symmetry group arises in the context of bosonic systems as its symmetry is implied by the commutation relations of the bosonic operators. As a first example consider the squeezing operator as given in equation (1.32) of the form

$$S(r) = e^{\frac{r}{2}(qp+pq)}. \tag{2.17}$$

The transformation of the quadrature operators can be obtained via the Hadamard lemma and the Baker-Campbell-Hausdorff formula namely

$$e^X Y e^{-X} = \sum_{k=0}^{\infty} \frac{1}{k!}[X, Y]_k, \tag{2.18}$$

where X, Y are linear Operators and $[X, Y]_k = [X, [X, Y]_{k-1}]$ with$[X, Y]_0 = Y$. This results in the following transformation matrix

$$\begin{pmatrix} q \\ p \end{pmatrix} \to \begin{pmatrix} e^{-r} & 0 \\ 0 & e^{r} \end{pmatrix} \begin{pmatrix} q \\ p \end{pmatrix}. \tag{2.19}$$

We can now check the symplecticity condition for the squeezing operator:

$$S^T \Omega S = \begin{pmatrix} e^{-r} & 0 \\ 0 & e^{r} \end{pmatrix} \begin{pmatrix} 0 & -1 \\ 1 & 0 \end{pmatrix} \begin{pmatrix} e^{-r} & 0 \\ 0 & e^{r} \end{pmatrix} = \Omega. \tag{2.20}$$

This discussion connects to the discussion of Gaussian unitaries, as the transformation matrix in equation (2.19) is symplectic. This means that Gaussian unitaries have a symplectic structure in Phase space. We want to emphasize that we are working in the Heisenberg picture, hence we are looking at the transformation of operators, not states. This is important, as the transformation matrices of various gates will not coincide with the transformation matrices of the states in a discrete variable context.

2.2.3 Universal quantum computation

In order to be able to perform universal quantum computation we need Clifford gates and a non Clifford gate, for example the T gate.

Continuous variable Clifford group

In the context of discrete variable quantum computation the Clifford group is the normalizer of the Pauli group, hence the group that contains operations that map stabilizers onto stabilizers. In the discrete variable context [10] the Clifford group is generated by the Hadamard gate, the S gate and the CNOT gate, i.e.

$$\mathcal{C} = \langle H, S, \mathrm{CNOT} \rangle. \tag{2.21}$$

The continuous variable counterparts of the generators of the discrete variable Clifford group are taken from the original GKP paper [11]):

1. Hadamard gate:

   $$H = e^{i\frac{\pi}{2}(q^2+p^2-I)}, \tag{2.22}$$

   This is a phase space rotation, where essentially the q, p axes are swapped. This gate is often referred to as the Fourier gate, as it corresponds to a Fourier transform on the phase space operators.

2. CNOT gate:

   $$\mathrm{CNOT} = e^{-ip_2q_1} \tag{2.23}$$

   This is a conditional displacement on two qubits. As this and the corresponding CZ gate are part of the title of this thesis they require special attention. This will be covered in chapters 3 and 4 as well as in section 2.3.

3. S gate:

   $$S = e^{\frac{i\pi}{2}q^2} \tag{2.24}$$

   Here it is important to note that the relation between $S^2 = Z$ from the discrete variable context does no longer hold, which means you cannot construct the logical Z operator as in equation (1.16) from the S gate. However the Clifford group must contain the logical operators. Therefore it is not sufficient to just give these three operators to generate the Clifford group in the context of GKP states.

As has been seen in the context of continuous variable quantum computation the definition of the Clifford group is more unclear. We define the continuous variable Clifford group as defined in [2].

Theorem 2.2.1 (Continuous Clifford group)**.** *The Clifford group for continuous variables $\mathcal{C}_{CV}$ is the semidirect product group $[HW(n)]Sp(2n, \mathbb{R})$,consisting of all phase-space translations along with all one-mode and two-mode squeezing transformations. This group is generated by inhomogeneous quadratic polynomials in the canonical operators.*

The theorem states that the group contains both elements from the groups discussed in section 2.2.1 and 2.2.2 is generated by Hamiltonians which are inhomogeneous polynomials of second order in the quadrature operators. This allows to draw a line to the discussion on Gaussian quantum information. There we considered unitaries, which have exponents which are quadratic in the quadrature operators. The semi-direct product of the Heisenberg Weyl group and the symplectic group ensures that both the logical operators (elements of the Heisenberg Weyl group) and H,S and CNOT (elements of the symplectic group) are in the Clifford group.

UQC

Now finally we can look at what is necessary to achieve Universal continuous variable quantum computation. As we have seen Clifford group generators are at most quadratic polynomials in the quadrature operators. The condition to extend this to universal quantum computation is given by the Lloyd Braunstein criterion [14] and goes as follows: "Simple linear operations such as translations, phase shifts, squeezers, and beam splitters, combined with some nonlinear operation such as a Kerr nonlinearity, suffice to enact to an arbitrary degree of accuracy Hamiltonian operators that are arbitrary polynomials over a set of continuous variables. This means that additionally to the gates introduced before we need one gate which has to be realized via a non linear transformation."
We discussed the most important gates in continuous variable systems and the tools to describe them properly. We will now proceed to go into more detail regarding two qubit gates and their realizations.

2.3 Two Qubit Gates

Two qubit gates are essential in enabling universal quantum computation. We investigated in the symplectic CNOT and CZ gates, as symplectic gates can be realized, via a sequence of operations, that are experimentally accessible.

2.3.1 Ideal CNOT and ideal CZ

We will first define the ideal GKP CNOT and CZ gate and calculate its action on ideal GKP state. The discrete variable versions have been discussed in chapter 1.1.2. We will return in chapter 3 to the action on a finite energy GKP qubit and compare the results to the ideal case.

CZ gate

The CZ gate is a two qubit gate, which performs a logical Z gate on the target qubit if the control qubit is in state $|1\rangle$.The CZ gate for GKP states is given by

$$CZ = e^{-iq_2q_1}, \tag{2.25}$$

The transformation of the CZ gate in the Heisenberg picture can again be obtained using the Hadamard lemma and reads

$$\begin{pmatrix} q_1 \\ p_1 \\ q_2 \\ p_2 \end{pmatrix} \rightarrow \begin{pmatrix} 1 & 0 & 0 & 0 \\ 0 & 1 & -1 & 0 \\ 0 & 0 & 1 & 0 \\ -1 & 0 & 0 & 1 \end{pmatrix} \begin{pmatrix} q_1 \\ p_1 \\ q_2 \\ p_2 \end{pmatrix}. \tag{2.26}$$

Note that this Matrix is different from the discrete variable matrix, which is given by

$$CZ = \begin{pmatrix} 1 & 0 & 0 & 0 \\ 0 & 1 & 0 & 0 \\ 0 & 0 & 1 & 0 \\ 0 & 0 & 0 & -1 \end{pmatrix} = |0\rangle\langle 0| \otimes I + |1\rangle\langle 1| \otimes \sigma_z, \tag{2.27}$$

where σ_z in this case stands for the discrete variable Pauli Z matrix, not the logical operator from section 1.1.3. This difference arises again because in continuous variable systems we are describing transformations in the Heisenberg picture, whereas in the discrete variable we are describing transformations of states, hence we are in the Schrödinger picture. We will now show that the discrete variable matrix can be obtained from the continuous variable definition of the CZ. To do so we apply the CZ gate to the ideal GKP computational basis states, as given in section 1.1.3
We will first show the behaviour of CZ gate on an ideal position eigenstate. To see the behaviour we use a trick already used before and expand our operator into a Taylor series

$$\mathrm{CZ}\,|q_1\rangle|q_2\rangle = e^{-iq_1q_2}|q_1\rangle|q_2\rangle = \sum_{n=0}^{\infty} \frac{(-i)^n}{n!}(q_1q_2)^n|q_1\rangle|q_2\rangle = e^{-iq_1q_2}|q_1\rangle|q_2\rangle. \tag{2.28}$$

This tells us that the CZ gate applied to a position eigenstate acts as a phase. Next, we note that the computational basis states are either superpositions of even or of odd $\sqrt{\pi}$ multiples of position eigenstates. This requires that the exponent in equation (2.28) either acquires the value of an even or an odd multiple of π. It follows that the state either assumes an additional phase of ± 1 and the value -1 is only assumed if both qubits are in an odd position eigenstate, meaning both qubits are in $|1\rangle$. Performing this transformation for all computational basis states gives the transformation matrix from equation (**??**).This shows that the correct behaviour for the CZ gate in the Schrödinger picture is obtained. However we want to emphasize that we obtain our discrete variable matrix representation only if you apply the CZ gate to the computational basis states. The computational basis states are only a subspace of all states in phase space.

CNOT gate

We can extend the discussion from the CZ to the CNOT gate. The transformation matrix for the CNOT gate is obtained if the Hadamard Lemma is applied to the quadrature operators with the gate given as in equation (2.23). The transformation matrix in this case becomes

$$\begin{pmatrix} q_1 \\ p_1 \\ q_2 \\ p_2 \end{pmatrix} \rightarrow \begin{pmatrix} 1 & 0 & 0 & 0 \\ 0 & 1 & 0 & -1 \\ 1 & 0 & 1 & 0 \\ 0 & 0 & 0 & 1 \end{pmatrix} \begin{pmatrix} q_1 \\ p_1 \\ q_2 \\ p_2 \end{pmatrix}. \tag{2.29}$$

The action on the ideal computational basis states can be obtained if the CNOT is projected into position space via $\langle x_1, x_2| CNOT |10\rangle$, where $|00\rangle$ could be any computational basis state. The CNOT in position space is given by

$$CNOT(x_1, x_2) = \mathbb{1} \otimes T_2(x_1), \tag{2.30}$$

where T_2 is a translation along the q axis of the second qubit. Applied to the computational $|10\rangle$ state we obtain in position space:

$$\begin{aligned} \langle x_1, x_2| CNOT |10\rangle &= \mathbb{1} \otimes T_2(x_1) \sum_{i,j} \delta(x_1 - (2i+1)\sqrt{\pi})\delta(x_2 - 2j\sqrt{\pi}) \\ &= \sum_{i,j} \delta(x_1 - (2i+1)\sqrt{\pi})\delta(x_2 - \underbrace{(2j - 2i - 1)}_{\text{odd}}\sqrt{\pi}) \\ &= \langle x_1, x_2|11\rangle \end{aligned} \tag{2.31}$$

Repeating this calculation for all computational basis state we obtain the desired behaviour of the CNOT. As mentioned before we so far looked at the action on an ideal GKP state. In a next step we are going to look at the effect of the ideal CZ and CNOT gates on finite energy GKP states.

Chapter 3

Results I: Finite energy effects of ideal two qubit GKP gates

3.0.1 Finite energy effects of ideal gates

We will elaborate on the finite energy effects using the CZ gate, and we are going to proceed in the following way. First we are going to calculate the effect of the CZ gate on a squeezed state, then on a displaced squeezed state and finally on a finite energy GKP state.
Let the subscripts $1, 2$ stand for the control and target qubit, $\Delta_i, i \in \{1, 2\}$ be the squeezing parameters for the state preparation for both states. The operator S is the squeezing operator as defined in equation (1.32), and T is the translation operator in q space $T(a)\left|q\right\rangle = \left|q-a\right\rangle$.

CZ on Squeezed State

We will first look at the wave functions before and after the gate in position space, and then repeat in momentum space. The calculation goes as follows:

1. Position space:

    (a) First write down a squeezed state:

$$\begin{aligned} S(-\log(\Delta_1)) \otimes S(-\log(\Delta_2)) \left|g\right\rangle_1 \otimes \left|g\right\rangle_2 &= \int_{-\infty}^{\infty} \frac{dq_1}{(\pi\Delta_1^2)^{\frac{1}{4}}} e^{-\frac{q_1^2}{2\Delta_1^2}} \int_{-\infty}^{\infty} \frac{dq_2}{(\pi\Delta_2^2)^{\frac{1}{4}}} e^{-\frac{q_2^2}{2\Delta_2^2}} \left|q_1\right\rangle \left|q_2\right\rangle \\ &= \left|\psi_0\right\rangle_1 \left|\psi_0\right\rangle_2 . \end{aligned} \tag{3.1}$$

    (b) In order to find the wave function in position space we must apply the properties of the δ distribution described in equation (1.9). The wave function is obtained by projecting $\psi(x_1, x_2) = \left\langle x_1, x_2 \middle| \psi_0 \right\rangle_1 \left|\psi_0\right\rangle_2$. We obtain:

$$\begin{aligned} \psi(x_1, x_2) &= \int_{\mathbb{R}^2} \frac{dq_1 dq_2}{(\pi\Delta_1^2)^{\frac{1}{4}}(\pi\Delta_2^2)^{\frac{1}{4}}} e^{-\frac{q_1^2}{2\Delta_1^2}} e^{-\frac{q_2^2}{2\Delta_1^2}} \delta(q_1 - x_1)\delta(q_2 - x_2) \\ &\propto e^{-\frac{x_1^2}{2\Delta_1^2}} e^{-\frac{x_2^2}{2\Delta_1^2}} . \end{aligned} \tag{3.2}$$

    The wave function is Gaussian as is expected from a squeezed state.

    (c) Apply the CZ gate to the squeezed state and find the wave function in the same manner as before.

$$\mathrm{CZ} \left|\psi_0\right\rangle_1 \left|\psi_0\right\rangle_2 = \int_{-\infty}^{\infty} \frac{dq_1}{(\pi\Delta_1^2)^{\frac{1}{4}}} e^{-\frac{q_1^2}{2\Delta_1^2}} \int_{-\infty}^{\infty} \frac{dq_2}{(\pi\Delta_2^2)^{\frac{1}{4}}} e^{-\frac{q_2^2}{2\Delta_2^2}} e^{-iq_1q_2} \left|q_1\right\rangle \left|q_2\right\rangle . \tag{3.3}$$

This then leads to the following wave function $\psi_{\mathrm{CZ}}(x_1, x_2) = \langle x_1, x_2|\mathrm{CZ}|\psi_0\rangle_1 |\psi_0\rangle_2$:

$$\begin{aligned}\psi_{\mathrm{CZ}}(x_1, x_2) &= \int_{\mathbb{R}^2} \frac{dq_1 dq_2}{(\pi\Delta_1^2)^{\frac{1}{4}}(\pi\Delta_2^2)^{\frac{1}{4}}} e^{-\frac{q_1^2}{2\Delta_1^2}} e^{-\frac{q_2^2}{2\Delta_1^2}} e^{-iq_1q_2}\delta(q_1 - x_1)\delta(q_2 - x_2) \\ &\propto e^{-\frac{x_1^2}{2\Delta_1^2}} e^{-\frac{x_2^2}{2\Delta_1^2}} e^{-ix_1x_2}.\end{aligned} \tag{3.4}$$

Equation (3.4) gives already an into what will happen to a finite energy GKP State in position space: The new factor from the CZ gate appears as a global phase and will therefore vanish in the accessible probability distribution $|\psi(x)|^2$.

2. Momentum space:

   (a) To go from position into momentum space, we use the properties defined in equation (1.7) and (1.9) and calculate:

$$|\psi_0\rangle_1 |\psi_0\rangle_2 = \frac{1}{(\pi\Delta_1^2)^{\frac{1}{4}}(\pi\Delta_2^2)^{\frac{1}{4}}} \int_{-\infty}^{\infty} dp_1 \int_{-\infty}^{\infty} dp_2 \mathcal{F}[\psi(x_1, x_2)] |p_1\rangle \otimes |p_2\rangle, \tag{3.5}$$

   where $\psi(x_1, x_2)$ is given as in equation (3.2).

   (b) We use the fact that the Fourier transform of a Gaussian is again Gaussian. We find:

$$\psi(p_1, p_2) \propto e^{-\frac{\Delta_1^2}{2}p_1^2} e^{-\frac{\Delta_2^2}{2}p_2^2}, \tag{3.6}$$

   which are Gaussians with variance Δ_i^{-2}.

   (c) After the gate we Fourier transform $\psi_{CZ}(x_1, x_2)$. We can perform the resulting integral either by substitution or by using Cauchy's integral theorem. We obtain the following result:

$$\psi_{\mathrm{CZ}}(p_1, p_2) \propto e^{-\frac{\Delta_1^2}{2(1+\Delta_1^2\Delta_2^2)}p_1^2} e^{-\frac{\Delta_2^2}{2(1+\Delta_1^2\Delta_2^2)}p_2^2} e^{-i\frac{\Delta_1^2\Delta_2^2}{1+\Delta_1^2\Delta_2^2}p_1p_2}. \tag{3.7}$$

   The most important thing to notice is the new factor $1 + \Delta_1^2\Delta_2^2 = \Delta_p^2$ appearing in every term, changing the amplitudes as well as the widths of the Gaussians. The phase is again global and can be ignored.

In Figure 3 we can see the marginals in p space of a traced out squeezed state centred around 0 before and after the logical CZ gate. The marginals stay almost unchanged. A small imperfection arises due to the factor Δ_p^2.

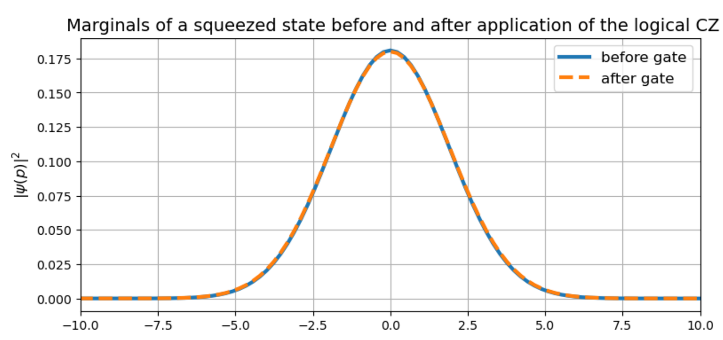

Figure 3.1: Marginals of a traced out squeezed state before and after application of the CZ gate. The input state was of the form $S(-\log(\Delta)) \otimes S(-\log(\Delta)) |g\rangle |g\rangle$ and $\Delta = 0.37$.

Before proceeding let us investigate further in the newly appearing factor, since it will be reappearing in most of the calculations from now on. The first thing to notice is that it will only appear as a denominator and that it is greater or equal than 1. This means:

$$\frac{\Delta_i^2}{\Delta_p^2} < \Delta_i^2, \tag{3.8}$$

where $\Delta_p^2 = 1 + \Delta_1^2\Delta_2^2$. This causes the exponents in p - space to decrease and reduces therefore also the quality of the state after the gate.

CZ on Displaced Squeezed State

Now we repeat the calculation for a displaced squeezed state, where we displace along the q direction in Phase Space. Assume that on state 1 we displace by an amount a and on state 2 by an amount b, where both quantities are real parameters.

1. First write down a general displaced squeezed state in q direction and define the operator $O = (T(a) \otimes T(b))(S(-\log(\Delta_1)) \otimes S(-\log(\Delta_2))$

$$O \left|g\right\rangle_1 \left|g\right\rangle_2 = \int_{-\infty}^{\infty} \frac{d\tilde{q}_1}{(\pi\Delta_1^2)^{\frac{1}{4}}} e^{-\frac{(\tilde{q}_1-a)^2}{2\Delta_1^2}} \int_{-\infty}^{\infty} \frac{d\tilde{q}_2}{(\pi\Delta_2^2)^{\frac{1}{4}}} e^{-\frac{(\tilde{q}_2-b)^2}{2\Delta_2^2}} \left|\tilde{q}_1\right\rangle \left|\tilde{q}_2\right\rangle = |\tilde{\psi}_0\rangle_1 |\tilde{\psi}_0\rangle_2 . \tag{3.9}$$

In the calculation above we performed the following substitution $q \to q + a = \tilde{q}$ and similarly for b, which means $dq = d\tilde{q}$. We obtain a squeezed state whose mean has been shifted away from 0. We can now apply the same techniques as in the sections above to find the wave functions in position and momentum space.

2. Position space: In position space we find the following wave function before the gate:

$$\psi(x_1, x_2) \propto e^{-\frac{(x_1-a)^2}{2\Delta_1^2}} e^{-\frac{(x_2-b)^2}{2\Delta_2^2}} . \tag{3.10}$$

This is just a displaced Gaussian as one would expect. If you now apply the CZ gate and perform the integrals you find the following form:

$$\psi_{CZ}(x_1, x_2) \propto e^{-\frac{(x_1-a)^2}{2\Delta_1^2}} e^{-\frac{(x_2-b)^2}{2\Delta_2^2}} e^{-ix_1x_2}. \tag{3.11}$$

This underlines once more that in position space the wave function does not change under application of the CZ gate up to a global phase.

3. Momentum Space: We again Fourier transform the wave functions before and after the gate. Before the gate we obtain

$$\psi(p_1, p_2) \propto e^{-\frac{\Delta_1^2}{2}p_1^2} e^{-\frac{\Delta_2^2}{2}p_2^2} e^{iap_1} e^{ibp_2}. \tag{3.12}$$

After the gate we Fourier Transform equation (3.11) to obtain

$$\psi_{CZ}(p_1, p_2) \propto e^{-\frac{\Delta_1^2}{2\Delta_p^2}(p_1-b)^2} e^{-\frac{\Delta_2^2}{2\Delta_p^2}(p_2-a)^2} e^{\frac{ia}{2\Delta_p^2}p_1} e^{\frac{ib}{2\Delta_p^2}p_2} e^{\frac{ip_1p_2\Delta_1^2\Delta_2^2}{2\Delta_p^2}} e^{\frac{-iab}{2\Delta_p^2}} \tag{3.13}$$

The first thing to note is, that compared to the expression before the gate the scaling factor in Δ_p^2 reappears. We can observe that a phase factor appears (the last exponential in the expression above) which depends solely on the shifts applied from the displacements. We observe that in momentum space the Gaussians are now shifted, depending on the shifts of the input in position space. However p_1 is shifted by the amount b which was the displacement in state 2 in q space and p_2 is shifted by the amount a which was the displacement in mode 1 in q space. We can see this behaviour also in Figure 4.
We have now acquired all necessary tools to calculate the change in the wave function of a finite Energy GKP state.

CZ on Finite Energy GKP states

We can use the calculations from above to find the effect of the CZ gate on a finite energy GKP state. We will restrict ourselves to the calculation for a finite computational basis state, namely the state $|00\rangle$. The position wave function of this state is given by:

$$\psi_{|00\rangle}(x_1, x_2) \propto \sum_{s_1, s_2 \in \mathbb{Z}} e^{-\frac{1}{2}\kappa_1^2(2s_1\sqrt{\pi})^2} e^{-\frac{1}{2}\kappa_2^2(2s_2\sqrt{\pi})^2} e^{-\frac{1}{2\Delta_1^2}(x_1-2s_1\sqrt{\pi})^2} e^{-\frac{1}{2\Delta_2^2}(x_2-2s_2\sqrt{\pi})^2}, \tag{3.14}$$

where κ_i is the envelope of the respective mode. Using that in position space the wave function of a displaced squeezed state does not change up to a global phase we can find:

$$\psi_{CZ|00\rangle}(x_1, x_2) \propto \sum_{s_1, s_2 \in \mathbb{Z}} e^{-\frac{1}{2}\kappa_1^2(2s_1\sqrt{\pi})^2} e^{-\frac{1}{2}\kappa_2^2(2s_2\sqrt{\pi})^2} e^{-\frac{1}{2\Delta_1^2}(x_1-2s_1\sqrt{\pi})^2} e^{-\frac{1}{2\Delta_2^2}(x_2-2s_2\sqrt{\pi})^2} e^{-ix_1x_2}, \tag{3.15}$$

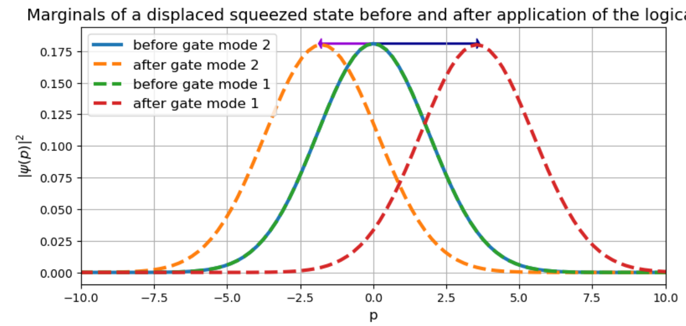

Figure 3.2: Marginals of traced out displaced squeezed states before and after application of the CZ gate. The input state was of the form $(T(a)S(-\log(\Delta))) \otimes (T(b)S(-\log(\Delta)))\,|g\rangle\,|g\rangle$ with $\Delta = 0.37$ and $a = \sqrt{\pi}, b = 2\sqrt{\pi}$. We can see that the after the gate the displacement of the first mode affects the state of the second mode. This is discussed in the main text.

which exhibits the same behaviour as seen for the displaced squeezed state in equation (3.11). In Figure 5 we can see that the marginals of the Wigner function before and after the gate do not change. This in accordance with our calculations.

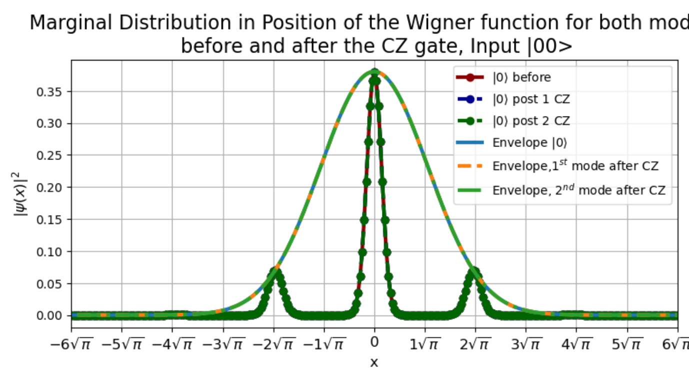

Figure 3.3: Marginals of the $|00\rangle$ state in q-space before and after the gate. The wave function does not change in the position quadrature.

When going to momentum space, we can observe that imperfections in the action of the gate affect solely the p quadrature. Before the gate the wave function in p space is given by

$$\psi_{|00\rangle}(p_1, p_2) \propto \sum_{s_1, s_2 \in \mathbb{Z}} e^{-\frac{1}{2}\kappa_1^2(2s_1\sqrt{\pi})^2} e^{-\frac{1}{2}\kappa_2^2(2s_2\sqrt{\pi})^2} e^{-\frac{\Delta_1^2}{2}p_1^2} e^{-\frac{\Delta_2^2}{2}p_2^2} e^{i(2s_1\sqrt{\pi})p_1} e^{i(2s_2\sqrt{\pi})p_2}. \tag{3.16}$$

This equation looks structurally exactly like the result for the displaced squeezed state in equation (3.12). This result can be simplified further, using the Poisson summation formula. The Poisson summation formula in its general form , for a function $f \in \mathcal{S}(\mathbb{R})$, with $\mathcal{S}(\mathbb{R})$ being the Schwartz space is given by:

$$\sum_{n \in \mathbb{Z}} f(n) = \sum_{k \in \mathbb{Z}} \hat{f}(k). \tag{3.17}$$

The summation formula therefore relates the summation over the function to the summation over the Fourier transformed function. For this we are Fourier transforming the running index, not the quadrature operator q or p. In the case of the displaced Gaussians [11] the Poisson summation formula can be written as

$$\sum_{n \in \mathbb{Z}} e^{-\pi a(n-b)^2} = \frac{1}{\sqrt{a}} \sum_{m \in \mathbb{Z}} e^{-\pi \frac{m^2}{a}} e^{2\pi i m b}. \tag{3.18}$$

If we separate the sums in our expression for the momentum wave function above and apply the Poisson summation formula we find the following values for the constants a_i, b_i on each mode, where the index i

marks the respective mode:

$$a_i = \frac{1}{2\kappa_i^2}, \qquad b_i = \frac{p_i}{\sqrt{\pi}}. \tag{3.19}$$

We can thus rewrite the expression for the wave function in the following compact form:

$$\psi(p_1, p_2) \propto e^{-\frac{\Delta_1^2}{2}p_1^2} e^{-\frac{\Delta_2^2}{2}p_2^2} \sum_{s_1, s_2 \in \mathbb{Z}} e^{-\frac{1}{2\kappa_1^2}(p_1 - s_1\sqrt{\pi})^2} e^{-\frac{1}{2\kappa_2^2}(p_2 - s_2\sqrt{\pi})^2}. \tag{3.20}$$

From the last equation we can see how the envelope of the state and the variance of the peaks change if we go from q to p quadrature, namely we can find that:

$$\kappa_i \to \Delta_i. \tag{3.21}$$

This relates the with of the envelope in q space to the width of the peaks in p space and vice versa and motivates the common choice of setting $\Delta = \kappa$ as this yields a symmetric state in both q and p direction. The wave function after the gate looks as following:

$$\begin{aligned} \psi_{CZ}(p_1, p_2) \propto \sum_{s_1, s_2 \in \mathbb{Z}} & e^{-\frac{1}{2}\kappa_1^2(2s_1\sqrt{\pi})^2} e^{-\frac{1}{2}\kappa_2^2(2s_2\sqrt{\pi})^2} e^{-\frac{\Delta_1^2}{2\Delta_p^2}(p_1 - 2s_2\sqrt{\pi})^2} e^{-\frac{\Delta_2^2}{2\Delta_p^2}(p_2 - 2s_1\sqrt{\pi})^2} \\ \times\, & e^{\frac{i(2s_1\sqrt{\pi})}{\Delta_p^2}p_1} e^{\frac{i(2s_2\sqrt{\pi})}{\Delta_p^2}p_2} e^{\frac{ip_1p_2\Delta_1^2\Delta_2^2}{\Delta_p^2}} e^{\frac{-i(2s_2\sqrt{\pi})(2s_1\sqrt{\pi})}{\Delta_p^2}}. \end{aligned} \tag{3.22}$$

We observe that the effective squeezing parameter appears in almost every term. This term creates an overall imperfection of the resulting state. Furthermore we can notice that this effective squeezing links the both sums as can be seen in the last term of the series above. Since this term is omnipresent in these calculation we are now making a detour into exploring this factor further to understand how much this affects the outcome of the gate. Next we can observe that we cannot separate one sum from the other, which makes a direct application of the Poisson summation formula impossible.
In Figure 6 we can see the marginals in p space of the Wigner function of the traced out modes of the logical $|00\rangle$ state before and after the logical CZ gate. We can see that that the shape of the marginals

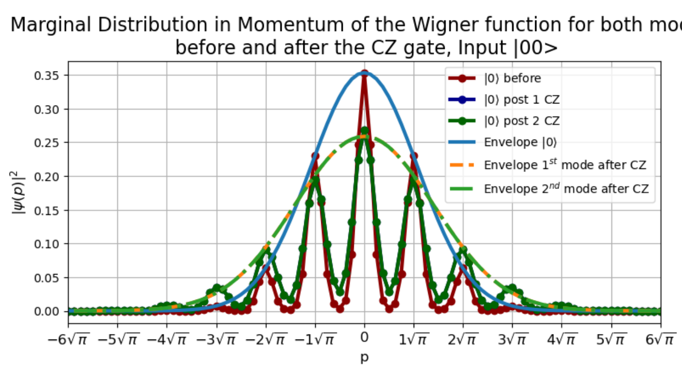

Figure 3.4: Marginals of the $|00\rangle$ state in p-space before and after the gate. A broadening of the envelope is observed as well as a lowering of the amplitude

under application of the gate changes. Since the marginals are in 1:1 correspondence with the wave function this also insinuates that the wave function changes. In the ideal case the wave function should stay ideally unchanged (since the $|00\rangle$ state should not change under application of the logical CZ). We observe that the ideal CZ gate induces finite energy effects on the states. To further quantify this equation we will analyse the effective squeezing parameter Δ_p.

The effective squeezing parameter Δ_p^2

The effective squeezing parameter $\Delta_p^2 = 1 + \Delta_1^2\Delta_2^2$ appears in every denominator of the wave function in p space after the CZ gate. Since this term is strictly greater than 1 it is therefore going to affect the quality of the resulting states. The parameters Δ_i^2 are typically chosen to be close to 0 as $\Delta \to 0$ corresponds to an infinitely squeezed state. This can be seen as a squeezed state with width Δ^2 is generated via the squeezing $S(-\log(\Delta))$. We can therefore Taylor expand this factor at $\Delta_1^2\Delta_2^2 = 0$. A typical squeezing is [17] $\Delta_i = 0.37$, therefore $\Delta_i^4 \approx 0.019$ and therefore this expansion is reasonable. We get

$$\frac{1}{\Delta_p^2}\bigg|_{\Delta_1^2\Delta_2^2=0} = 1 - (\Delta_1\Delta_2)^2 + (\Delta_1\Delta_2)^4 + \mathcal{O}((\Delta_1\Delta_2)^6). \tag{3.23}$$

The first thing that comes up in this calculation is, that the expression is constant up to first order and the second order contribution, inserting the value $\Delta = 0.37$, is of the order 10^{-2}. As stated however before, in the low squeezing limit, higher order terms start to give non negligible contributions. A correct choice of the squeezing parameters is therefore essential to retain a high quality GKP state even after the gate. We will discuss what happens to the wave function if we neglect the effective squeezing parameter.

Continuation of the discussion of the wavefunction

Setting the effective squeezing parameter equal to 1, we can now further simplify our wave function from equation (3.22). The wave function is now given by

$$\psi_{CZ}(p_1,p_2) \propto \sum_{s_1,s_2\in\mathbb{Z}} e^{-\frac{1}{2}\kappa_1^2(2s_1\sqrt{\pi})^2} e^{-\frac{1}{2}\kappa_2^2(2s_2\sqrt{\pi})^2} e^{-\frac{\Delta_1^2}{2}(p_1-2s_2\sqrt{\pi})^2} e^{-\frac{\Delta_2^2}{2}(p_2-2s_1\sqrt{\pi})^2} e^{i(2s_1\sqrt{\pi})p_1} e^{i(2s_2\sqrt{\pi})}, \tag{3.24}$$

where we omitted the global phase and the relative phase term containing both running indices, since now it evaluates to one per term. This looks already similar to the wave function before the gate however with 1 major difference. The terms containing the envelope, hence the terms which are squared in the p operators are shifted by $2\sqrt{\pi}$. We can use the Poisson summation formula to simplify this result even more. Using the Poisson summation formula we arrive at the following wave function after the gate

$$\psi_{CZ}(p_1,p_2) \propto e^{-\frac{\Delta_1^2}{2}p_1^2} e^{-\frac{\Delta_2^2}{2}p_2^2} \sum_{s_1,s_2\in\mathbb{Z}} e^{-\frac{1}{\kappa_1^2+\Delta_2^2}(p_1-ip_2\Delta_2^2+\sqrt{\pi}s_1)^2} e^{-\frac{1}{\kappa_2^2+\Delta_1^2}(p_2-ip_1\Delta_1^2+\sqrt{\pi}s_2)^2}. \tag{3.25}$$

As we can see this has the same structure as the wave function before the gate. We observe that the individual peaks under the envelope have been broadened with a width of $\kappa_i^2 \to \kappa_i^2 + \Delta_j^2, i \neq j$, while the envelope itself seems to stay untouched. Although the broadening of the peaks under the envelope is in accordance with the simulations discussed in chapter 4.0.5 the unchanged envelope is not. We want therefore to emphasise that setting the effective squeezing parameter equal to one, while leaving the other parameters unchanged has solely demonstrational purposes, since $\Delta_p = 1$ implies $\Delta_i = 0$. This means $\Delta_p = 1$ implies the infinite squeezing limit.
We have seen that the ideal CZ gate creates finite energy errors on a finite energy GKP state. The marginals in q space remain unchanged, however in p space a broadening of the envelope as well as a broadening of the peaks under the envelope is observed. We have given an explicit formula for the wave function before and after the CZ gate. We will now try to quantify the change in the envelope.

The envelope change

We wanted to quantify the change in the envelope of the states under application of the CZ using the following steps:

1. Perform the partial trace on the state after the gate to obtain the expression for a single qubit.
2. Fourier transform the resulting reduced density matrix to obtain a result in both p and q space.
3. Calculate the diagonals of the reduced density matrix. The diagonals of the reduced density matrix correspond to the occupation probabilities and are therefore in 1:1 correspondence with the marginals of the Wigner functions.

The partial trace is basis independent, therefore we can choose to perform the partial trace in the q basis. We will first show the calculation on a general state and then return to our specific example from above. Assume we are in a state given by:

$$|\psi\rangle = \int dq_1 dq_2 \psi(q_1,q_2) |q_1\rangle |q_2\rangle . \tag{3.26}$$

The corresponding density matrix is given by

$$\rho = \int dq_1 dq_1' dq_2 dq_2' \left[\psi^*(q_1', q_2')\psi(q_1, q_2)\right] |q_1\rangle |q_2\rangle \langle q_1'| \langle q_2'| \,. \tag{3.27}$$

If we want to get rid of the first subsystem, we must sum over the basis vectors of the first subsystem. We can thus write the reduced density matrix as

$$\rho_2 = \int dq_1'' \int dq_1 dq_1' dq_2 dq_2' \langle q_1''| \psi(q_1, q_2) |q_1\rangle \langle q_1'| \psi^*(q_1', q_2') |q_1''\rangle |q_2\rangle \langle q_2'| \,, \tag{3.28}$$

which can be rewritten as

$$\rho_2 = \int dq_1'' \int dq_1 dq_1' dq_2 dq_2' \psi(q_1, q_2)\psi^*(q_1', q_2')\delta(q_1 - q_1'')\delta(q_1' - q_1'') |q_2\rangle \langle q_2'| \,. \tag{3.29}$$

We can now get rid of the delta functions by collapsing the corresponding integrals and find

$$\int dq_2 dq_2' \left[\int dq_1 \psi^*(q_1, q_2)\psi(q_1, q_2')\right] |q_2\rangle \langle q_2'| \,. \tag{3.30}$$

By performing the integral in the square brackets we can find the reduced density matrix of the second subsystem in terms of the position eigenstate basis. If we then want to find the occupation probability for the reduced state as a function of position we set $q_2 = q_2'$. To obtain the result in p space we can insert two identities as in equations (1.8),(1.9).
We can now perform this calculation explicitly for our states $|00\rangle$ and $CZ\,|00\rangle$ from the discussion before. We can take the wave function after the CZ gate in equation (3.15) and write the corresponding state by summing over all position eigenstates to obtain

$$CZ\,|00\rangle \propto \sum_{s_1, s_2 \in \mathbb{Z}} e^{-\frac{1}{2}\kappa_1^2(2s_1\sqrt{\pi})^2} e^{-\frac{1}{2}\kappa_2^2(2s_2\sqrt{\pi})^2} \int dq_1 dq_2 e^{-\frac{1}{2\Delta_1^2}(q_1 - 2s_1\sqrt{\pi})^2} e^{-\frac{1}{2\Delta_2^2}(q_2 - 2s_2\sqrt{\pi})^2} e^{-iq_1q_2} |q_1\rangle |q_2\rangle \,. \tag{3.31}$$

We can now use the algorithm above to find the reduced density matrix. The full density matrix is given by:

$$\begin{aligned}\rho_{2,CZ|00\rangle} \propto &\sum_{s_1,s_2,s_3,s_4 \in \mathbb{Z}} e^{-\frac{1}{2}\kappa_1^2(2s_1\sqrt{\pi})^2} e^{-\frac{1}{2}\kappa_1^2(2s_3\sqrt{\pi})^2} e^{-\frac{1}{2}\kappa_2^2(2s_2\sqrt{\pi})^2} e^{-\frac{1}{2}\kappa_1^2(2s_4\sqrt{\pi})^2} \times \int dq_1 dq_1' dq_2 dq_2' \\ &e^{-\frac{1}{2\Delta_1^2}(q_1 - 2s_1\sqrt{\pi})^2} e^{-\frac{1}{2\Delta_1^2}(q_1' - 2s_3\sqrt{\pi})^2} e^{-\frac{1}{2\Delta_2^2}(q_2 - 2s_2\sqrt{\pi})^2} e^{-\frac{1}{2\Delta_2^2}(q_2' - 2s_4\sqrt{\pi})^2} e^{-iq_1q_2} e^{iq_1'q_2'} |q_1\rangle |q_2\rangle \langle q_1'| \langle q_2'| \,.\end{aligned} \tag{3.32}$$

We can perform now the partial trace by computing the integral in the square brackets from equation (3.30), which yields the reduced density matrix

$$\begin{aligned}\rho_{2,CZ|00\rangle} \propto &\sum_{s_1,s_2,s_3,s_4 \in \mathbb{Z}} e^{-\frac{1}{2}\kappa_1^2(2s_1\sqrt{\pi})^2} e^{-\frac{1}{2}\kappa_1^2(2s_3\sqrt{\pi})^2} e^{-\frac{1}{2}\kappa_2^2(2s_2\sqrt{\pi})^2} e^{-\frac{1}{2}\kappa_1^2(2s_4\sqrt{\pi})^2} \\ &\times \int dq_2 dq_2' e^{-\frac{(\sqrt{\pi}(s_1 - s_3)^2)}{\Delta_1^2}} e^{-\frac{\Delta_1^2}{4}(q_2 - q_2')^2} e^{-\frac{1}{2\Delta_2^2}(q_2 - 2s_2\sqrt{\pi})^2} e^{-\frac{1}{2\Delta_2^2}(q_2' - 2s_4\sqrt{\pi})^2} e^{i\sqrt{\pi}(s_1 + s_3)(q_2 - q_2')} |q_2\rangle \langle q_2'| \,.\end{aligned} \tag{3.33}$$

Setting $q_2 = q_2'$ and find the probabilities

$$\begin{aligned}\rho_{2,CZ|00\rangle}(q_2, q_2) \propto &\sum_{s_1,s_2,s_3,s_4 \in \mathbb{Z}} e^{-\frac{1}{2}\kappa_1^2(2s_1\sqrt{\pi})^2} e^{-\frac{1}{2}\kappa_1^2(2s_3\sqrt{\pi})^2} e^{-\frac{1}{2}\kappa_2^2(2s_2\sqrt{\pi})^2} e^{-\frac{1}{2}\kappa_1^2(2s_4\sqrt{\pi})^2} \\ &\times e^{-\frac{1}{2\Delta_2^2}(q_2 - 2s_2\sqrt{\pi})^2} e^{-\frac{1}{2\Delta_2^2}(q_2 - 2s_4\sqrt{\pi})^2} e^{-\frac{(\sqrt{\pi}(s_1 - s_3)^2)}{\Delta_1^2}} \,.\end{aligned} \tag{3.34}$$

By splitting the sums we can finally write this as the following expression:

$$\rho_{2,CZ|00\rangle}(q_2, q_2) \propto \sum_{s_1, s_3 \in \mathbb{Z}} (...) \sum_{s_2, s_4 \in \mathbb{Z}} e^{-\frac{1}{2}\kappa_2^2(2s_2\sqrt{\pi})^2} e^{-\frac{1}{2}\kappa_1^2(2s_4\sqrt{\pi})^2} e^{-\frac{1}{2\Delta_2^2}(q_2 - 2s_2\sqrt{\pi})^2} e^{-\frac{1}{2\Delta_2^2}(q_2 - 2s_4\sqrt{\pi})^2} \,, \tag{3.35}$$

which is up to normalization the exact same expression for the marginals as if we were to look at the marginals before the gate. This corresponds to the result that the marginals in q-space do not change before and after the gate.
We can proceed to look at what happens in p- space. We can insert two identities into our reduced density matrix in q- space, which essentially enables a Fourier transform in q_2 and an inverse Fourier transform in q_2'. We can then again look at the diagonal elements by setting $p_2 = p_2'$, which gives us the marginals in p space. We obtain the final result for the diagonal elements of the reduced density matrix:

$$\begin{aligned}\rho^2_{2,CZ|00\rangle}(p_2,p_2) \propto e^{-\frac{\Delta_2^2}{\Delta_p^2}p_2^2} \sum_{s_1,s_2,s_3,s_4\in\mathbb{Z}} & e^{-\frac{1}{2}\kappa_1^2(2s_1\sqrt{\pi})^2} e^{-\frac{1}{2}\kappa_1^2(2s_3\sqrt{\pi})^2} e^{-\frac{1}{2}\kappa_2^2(2s_2\sqrt{\pi})^2} e^{-\frac{1}{2}\kappa_2^2(2s_4\sqrt{\pi})^2} \\ \times\, & e^{-\frac{\pi(s_1-s_3)^2}{\Delta_1^2\Delta_p^2}} e^{-\frac{\Delta_1^2\pi}{\Delta_p^2}(s_2-s_4)^2} e^{\frac{2i\sqrt{\pi}p_2(s_2-s_4)}{\Delta_p^2}} e^{-\frac{2i\pi(s_1-s_3)(s_2-s_4)}{\Delta_p^2}} e^{\frac{2\sqrt{\pi}p_2\Delta_2^2(s_1+s_3)}{\Delta_p^2}} e^{-\frac{2\pi\Delta_2^2(s_1^2+s_3^2)}{\Delta_p^2}},\end{aligned} \tag{3.36}$$

where the effective squeezing parameter is the same as discussed before. We want to emphasize that we cannot reduce these sums by equalizing the summation indices $s_1 = s_3$ and $s_2 = s_4$, which we checked numerically. We can now compare this to the marginals before the gate. We can obtain these marginals by taking the density matrix of state $|00\rangle$ and look at the diagonal elements. These will take the form

$$\rho_{2,|00\rangle}(p_2,p_2) \propto e^{-\Delta_2^2 p_2^2} \sum_{s_1,s_3\in\mathbb{Z}} (...) \sum_{s_2,s_4\in\mathbb{Z}} e^{-\frac{1}{2}\kappa_2^2(2s_2\sqrt{\pi})^2} e^{-\frac{1}{2}\kappa_2^2(2s_4\sqrt{\pi})^2} e^{2i\sqrt{\pi}p_2(s_2-s_4)}. \tag{3.37}$$

We can see that the prefactor and the summand also appear in the partial trace after the gate, up to a change of an effective squeezing parameter in the exponent. However, it is also apparent that error terms appear in the partial trace after the gate. Now we have to try to extract the width of the envelope of the marginals. Before the gate we know that the envelope of the wave function is of the form $\propto e^{-\frac{\Delta^2}{2}p^2}$, hence the marginals are of the form $\propto e^{-\Delta^2 p^2}$. At the time of writing this thesis we could not find a way to extract the analytical expression for the envelope from the expression above, therefore further research in that area is required. It can be seen however that a change in the marginals is obtained under the application of the CZ gate, and we can indeed expect for the envelope of the states to change.

Numerical analysis of the envelope

We will now discuss the change of the envelope numerically. We want to quantify the numerical change of the envelope under application of the CZ gate in p space. To do so we initialized different $|00\rangle$ states for $\Delta_i = \kappa_i$ in a range between $[0.3, 0.8]$ and applied the CZ gate to it. We then traced out one mode, calculated the Wigner function for the reduced state and marginalized the state in q to obtain the marginals in p. We then fitted a Gaussian of the form

$$Env(A,b,c) = Ae^{-\frac{(x-b)^2}{2c}},$$

to the maxima of the peaks of our resulting state. By keeping track of the parameter c we can see how the envelope of the state changes under application of the CZ gate. In Figure 7 we can see the behaviour of the variance c before and after the gate as a function of κ. For this simulation we defined several two qubit $|00\rangle$ states with a variable κ and a fixed $\Delta = 0.37$. We can observe the following things: First we can see that the width of the envelope changes after the gate. However it seems that after a high enough κ the width returns to its original value before the gate. From our discussion in the chapter before on the relation between κ and Δ we would expect that the width of the envelope in p space should stay unchanged as Δ is fixed for our simulations. This is not the observed behaviour. Further investigation is needed in this subject to find a closed solution.

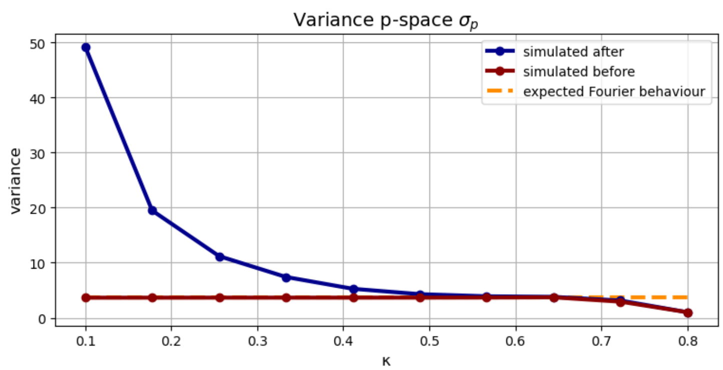

Figure 3.5: Change of the envelope of the state in p space under application of the CZ gate.

Chapter 4

Results II: Implementations of symplectic two qubit gates

So far we considered only ideal two qubit gates and their effect on finite energy states. We will now proceed to investigate on how to implement such gates in a more realistic experimental setting. In particular, we will consider an implementation of a logical CNOT as given in the work of Tzitrin et al. [25] and a novel approximate implementation of a logical CZ. We have already seen that symplectic gates can be implemented using linear optical elements such as beamsplitters and squeezers. This chapter is structured as follows: We will first give an introduction to the necessary mathematical tools to find analytical results for our implementations, we will then proceed to define the relevant optical elements and finally we are going to analyse these schemes and compare them.

4.1 Methods for gate decomposition

4.1.1 Mathematical tools

In this section, we are going to work in the Heisenberg picture of quantum mechanics and are therefore looking at transformations of operators, not states. The effect of an operator on another operator is given by conjugation and can be calculated using the Baker Campbell Hausdorff formula, which we have already seen in the chapter 2.2.2 We have seen how to apply this formula in the case of the squeezing operator, the phase space representation of the CNOT and the CZ can be found in a similar procedure. The next important tool that has to be introduced is the Bogoliubov transformation[4], which allows to map one pair of bosonic operators to another pair of bosonic operators. We therefore have to return to the Fock space representation of the bosonic Hilbert space. Consider two sets of bosonic creation and annihilation operators, which are connected via the following transformation:

$$b^\dagger = ua + va^\dagger \tag{4.1}$$

$$b = u^* a^\dagger + v^* a, \tag{4.2}$$

where $u.v \in \mathbb{C}$. We want this relation to be canonical, hence the following relation has to hold:

$$[b^\dagger, b] = [a^\dagger, a] = 1. \tag{4.3}$$

Direct calculation gives $|u|^2 - |v|^2 = 1$, which results in variables that can be parametrized by the hyperbolic functions

$$u = e^{i\theta_1} \cosh(x) \tag{4.4}$$

$$v = e^{i\theta_2} \sinh(x). \tag{4.5}$$

This transformation is symplectic, as the transformation can be written in the following matrix notation:

$$\begin{pmatrix} b^\dagger \\ b \end{pmatrix} \begin{pmatrix} e^{i\theta_1}\cosh(x) & e^{i\theta_2}\sinh(x) \\ e^{-i\theta_1}\cosh(x) & e^{-i\theta_2}\sinh(x) \end{pmatrix} \begin{pmatrix} a^\dagger \\ a \end{pmatrix}, \tag{4.6}$$

which conserves the symplectic form. We will need such transformations in order to decompose the logical gates into elements, which can be used in an experimental setting. More details can be found in textbooks, for example in reference [3]. The decomposition we are going to use is theorized in Braunstein et al. [6] and is given by the following theorem.

Theorem 4.1.1 (Bloch Messiah decomposition)**.** *For a general linear unitary Bogoliubov transformation of the form*

$$b_j = \sum_k (A_{jk} a_k + B_{jk} a_k^\dagger) + \beta_j \tag{4.7}$$

where a_j ,b_j are bosonic annihilation operators, the matrices A and B may be decomposed into a pair of unitary matrices V and V and a pair of non-negative diagonal matrices A_D and B_D satisfying

$$A_D^2 = B_D^2 + \mathbb{1}, \tag{4.8}$$

with $\mathbb{1}$ the identity matrix, by

$$A = U A_D V^\dagger \tag{4.9}$$

$$B = U B_D V^T \tag{4.10}$$

This theorem shows, that any operator inducing a linear unitary operator Bogoliubov transformation can be decomposed into four separate operators, of which two are diagonal. We will now see by introducing the relevant linear optical elements how this can be put into context for a GKP qubit gate.

4.1.2 Linear optical elements

For our purposes it is sufficient to understand some important one- and two mode operations, which are the squeezer and beamsplitter respectively. We have already seen in the beginning of this thesis, that the squeezing operation is given by

$$S(r) = \exp\big(\frac{r}{2}(qp + pq)\big) = \exp\big(\frac{r}{2}(a^2 - a^{\dagger 2})\big). \tag{4.11}$$

The squeezing operator induces the following transformation on the Fock and quadrature operators

$$a \to (\cosh(r))a - (\sinh(r))a^\dagger \tag{4.12}$$

$$\begin{pmatrix} q \\ p \end{pmatrix} \to \begin{pmatrix} e^{-r} & 0 \\ 0 & e^r \end{pmatrix} \begin{pmatrix} q \\ p \end{pmatrix}. \tag{4.13}$$

We have seen that this transformation is symplectic. In physical terms, a squeezed state enhances the resolution in phase space of one quadrature, while reducing the resolution in the other quadrature.
The beamsplitter on the other hand is a two mode operation, which can vary in its definition from paper to paper, however we will stick to the following two definitions, where the first is going to be used in the decomposition for the CZ and the second is going to be used in the decomposition of the CNOT.

$$BS_{CZ}(\theta) = \exp\big(\frac{i\theta}{2}(q_1 q_2 + p_1 p_2)\big) = \exp\big(\frac{i\theta}{2}(a_1^\dagger a_2 + a_1 a_2^\dagger)\big) \tag{4.14}$$

$$BS_{CNOT}(\theta) = \exp\big(i\theta(p_1 q_2 - q_1 p_2)\big) = \exp\theta(a_1 a_2^\dagger - a_1^\dagger a_2)\big). \tag{4.15}$$

The beamsplitter operation is again symplectic in phase space, this can be seen as it is at most quadratic in the quadrature operators and therefore symplectic. The phase space representation of the first version of the beamsplitter is for instance given by the following transformation

$$\begin{pmatrix} q_1 \\ p_1 \\ q_2 \\ p_2 \end{pmatrix} \to \begin{pmatrix} \cos\frac{\theta}{2} & 0 & 0 & \sin\frac{\theta}{2} \\ 0 & \cos\frac{\theta}{2} & \sin\frac{\theta}{2} & 0 \\ 0 & \sin\frac{\theta}{2} & \cos\frac{\theta}{2} & 0 \\ \sin\frac{\theta}{2} & 0 & 0 & \cos\frac{\theta}{2} \end{pmatrix} \begin{pmatrix} q_1 \\ p_1 \\ q_2 \\ p_2 \end{pmatrix}. \tag{4.16}$$

We can now return to the Bloch-Messiah decomposition, introduced in the section before. For a proper set of squeezing and beamsplitter parameters, a two mode unitary operation can be decomposed into a beamplitter, followed by the parallel application of two squeezers and another beamsplitter interaction. This allows us to construct decompositions, which do not approximate the desired gate, but can exactly reproduce the desired gate. This decomposition is going to be used for the CNOT gate, however not for the CZ gate, as this will be an approximation not an exact gate.

4.1.3 Quality measures of GKP gates

In the next sections, we want to discuss how well do these gates perform, when applied to finite energy GKP states. It is therefore important to introduce the measures that are being investigated to test the quality of the resulting state. We will look at the Fidelity of the state, the Holevo phase variance and the effective squeezing parameters. For further details about these concepts, we refer the reader to the work of D. Weigand [8].

The fidelity

The fidelity of two quantum states measures how big the overlap of one state is to the other one. In general the fidelity for two density matrices ρ, σ is defined as

$$F(\sigma, \rho) = \left(Tr\left(\sqrt{\rho}\sigma\sqrt{\rho}\right)\right)^2, \tag{4.17}$$

which for two pure states reduces to the well known overlap

$$F(|\psi\rangle, |\phi\rangle) = |\langle\psi|\phi\rangle|^2. \tag{4.18}$$

Weigand states in this thesis that for GKP states the fidelity tends to underestimate the quality of the state and is therefore not the best measure of the quality of a GKP state. Therefore we will also investigate in other measures quantifying the quality of a GKP state.

The Holevo phase variance

Before introducing the measures that are about to come we want to make a quick detour regarding notation. So far we denoted in q space the envelope of the state as κ^{-2} and the width of the peaks under the envelope as Δ and stated that those two had an inverse relation as seen in equation (91) in p space. We will now call the widths of the peaks under the envelope in $q(p)$- space as $\Delta_q(\Delta_p)$. Since we have also seen that the envelope in p space under application of the CZ gate changes, while the peaks under the envelope in q space do not change we want to emphasize that in this case the transformation relations between envelope and peaks under the envelope do not necessarily hold and hence

$$\Delta_p \neq \frac{1}{\Delta_q}.$$

The Holevo phase variance is given by

$$\sigma_H = \sqrt{|Tr(\rho U)|^{-2} - 1}. \tag{4.19}$$

It measures how close a state ρ is on being an eigenstate of a unitary operator U. Since we want our states to remain in the code space, we want to know how close our states after application of a gate are to being eigenstates of the stabilizers S_x, S_z. For a perfect eigenstate the Holevo phase variance vanishes. This is the case for the ideal GKP codewords as defined at the beginning of this thesis. It is worthwhile noting that we are considering two qubit states, but we are interested on how the Holevo phase variance changes for one qubit, hence the relevant unitaries in our case are of the form $S_i \otimes \mathbb{1}$ for the control qubit and $\mathbb{1} \otimes S_i$ for the target qubit.
However this measure can be used to extract the width and the mean of the peaks under the envelope. We will see this in the next subsection.

4.1.4 Effective squeezing and effective mean

We can calculate explicitly the expectation value in the square-root of the Holevo phase variance. If we for instance consider as an input state a displaced logical 0 state, we find:

$$Tr(S_z |\psi\rangle\langle\psi|) = e^{i2\sqrt{\pi}\mu} e^{-\Delta^2\pi}, \tag{4.20}$$

which if taken the argument or the modulus gives us the expressions

$$\mu_q = \frac{Arg(Tr(|\psi\rangle\langle\psi|))}{2\sqrt{\pi}} \tag{4.21}$$

$$\Delta_q = \sqrt{\frac{1}{2\pi}\log\left(\frac{1}{|Tr(|\psi\rangle\langle\psi|)|^2}\right)}. \tag{4.22}$$

An analogous expression can be found, if we apply the S_x stabilizer. This measure allows us to measure the change of the position and widths of the peaks before and after the application of the gate. The effective squeezing parameters and the Holevo phase variance are connected. This can be seen if we consider states which are close to ideal GKP states, meaning $\Delta \to 0$. In this case, we can expand the logarithm to find

$$\Delta_q = \frac{1}{\sqrt{2\pi}} \sigma_H. \tag{4.23}$$

4.1.5 Numerical methods

Before diving into the results of the different implementations of the 2 qubit gates, we want to present the numerical methods used to obtain the results. We used for the state preparation the method using the θ-functions introduced my Mensen et al.[16] and also described in the beginning of this thesis. The state preparation, Wigner functions calculation and the error-correction processes are implemented using the CVsim.jl package in Julia[20], whereas all simulations were done using the QuantumOptics.jl package [13]. The gates were not simulated using their exponential forms, but using the Schrödinger equation. This is explained below on the example of the CZ gate. The CZ gate as we have seen before is given by

$$CZ = e^{-iq_1q_2}$$

and is thus generated by a Hamiltonian of

$$H = q_1q_2. \tag{4.24}$$

This Hamiltonian is time independent, hence we can apply this Hamiltonian to the Schrödinger equation

$$i\partial_t \left|\psi\right\rangle = H \left|\psi\right\rangle, \tag{4.25}$$

for an input state $|\psi\rangle$ and integrate this equation out explicitly and obtain

$$|\psi(t)\rangle = e^{-iHt} \left|\psi_0\right\rangle. \tag{4.26}$$

By numerically integrating this equation between 0 and 1 and keeping only the final step of the integration, you obtain exactly the action of the CZ gate on an input state.

4.2 The approximate CZ gate

We will first look at the approximate CZ gate. As opposed to the Bloch-Messiah decomposition, this approximates the CZ gate by concatenating two parallel squeezers, followed by a beamsplitter and then by an antisqueezer. This can be seen by the circuit in Figure 8. The beamsplitter is being conjugated with

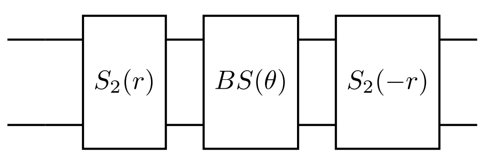

Figure 4.1: Decomposition of the approximate CZ gate. A beamsplitter is conjugated with two parallel single mode squeezers.

two parallel squeezing operations. We already know how squeezing operator transform the quadrature operators. We can therefore write the approx. CZ gate as a single exponential. This gives us two different expressions for the approximate CZ gate as seen in equation (4.27). We will refer to the single exponential as the full gate and the decomposition as the decomposed gate. The relevant equations are:

$$CZ_{\text{approx}} = e^{\frac{i\theta}{2}(e^{2r}q_1q_2 + e^{-2r}p_1p_2)} \tag{4.27}$$

$$CZ_{\text{approx}} = S_2(r)BS(\theta)S_2(-r), \tag{4.28}$$

where $S_2(r) = S(r) \otimes S(r)$. If we look at the full gate we can see that the first term looks similar to the exponent in the logical CZ, whereas the second term is a error that we want to vanish. To see what conditions are necessary for this gate to converge to the ideal CZ gate we can go into phase space and find the transformation of the quadrature operators under this gate. By applying the Baker-Campbell-Hausdorff formula we obtain the following matrix:

$$\begin{pmatrix} q_c \\ p_c \\ q_t \\ p_t \end{pmatrix} \rightarrow \begin{pmatrix} \cos\frac{\theta}{2} & 0 & 0 & e^{-2r}\sin\frac{\theta}{2} \\ 0 & \cos\frac{\theta}{2} & -e^{2r}\sin\frac{\theta}{2} & 0 \\ 0 & e^{-2r}\sin\frac{\theta}{2} & \cos\frac{\theta}{2} & 0 \\ -e^{2r}\sin\frac{\theta}{2} & 0 & 0 & \cos\frac{\theta}{2} \end{pmatrix} \begin{pmatrix} q_c \\ p_c \\ q_t \\ p_t \end{pmatrix}. \tag{4.29}$$

This matrix is symplectic. If we now recall the form of the ideal CZ gate from equation (2.26) and compare the matrix elements, we can find the following relation between the squeezing strength on the squeezers and the beamsplitter angle that has to hold for convergence to the ideal gate if $r \to \infty$:

$$e^{2r}\sin\frac{\theta}{2} = 1 \Leftrightarrow \theta(r) = 2\arcsin\left(e^{-2r}\right). \tag{4.30}$$

This relation is crucial for the understanding of the approximate CZ gate, therefore it is necessary to get a good understanding of its behaviour. We can plot the behaviour of the beamsplitter angle as a function of the squeezer, this can be seen in Figure 9.

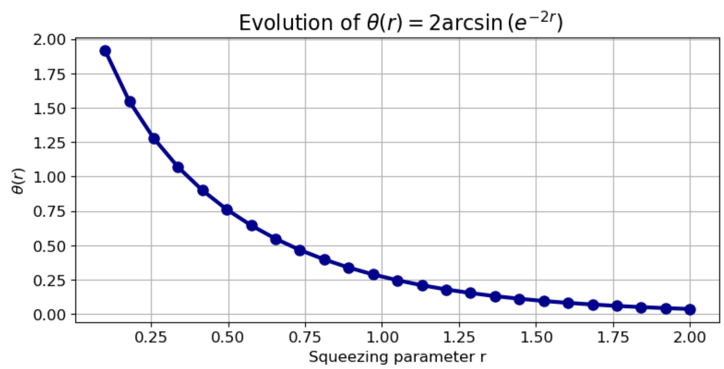

Figure 4.2: Beamsplitter parameter as a function of the squeezing strength.

We observe that this goes to 0 as r approaches infinity and diverges as r goes to 0. Note that we have two ways of examining the convergence in terms of the squeezing, we can look at it as a convergence in r or in $\Delta = e^{-r}$. We have to be careful though as $r \to \infty \Leftrightarrow \Delta \to 0$. If we apply the transformation to go into Δ-space our relation from before simplifies to

$$\theta(-\log(\Delta)) = 2\arcsin\left(\Delta^2\right). \tag{4.31}$$

We can now expand this equation around $\Delta = 0$ and find the following asymptotic behaviour

$$\theta(-\log(\Delta))\big|_{\Delta=0} = 2\Delta^2 + \mathcal{O}(\Delta^6), \tag{4.32}$$

which gives a quadratic convergence in Δ space if $\Delta \to 0$. We can now look at how the diagonal and off-diagonal terms in the approximate CZ gate behave if we apply the relations found above, this can be seen in figure 10. We see that the values saturate to the desired values after some squeezing is applied. This gives an intuition, that the gate, although being approximate, converges numerically to the ideal gate for squeezings $r \approx 1$. One thing that we want to emphasize here is that this gate works, because of the connection between r and θ in equation (4.30). While one parameter goes to infinity, the other goes to 0 and they balance each other out. This works if the full gate is considered. If however we consider the decomposed gate, numerical problems can arise (analytically these methods are completely equivalent). In the decomposed gate, we apply sequentially the squeezer and the beamsplitter. We have seen that the beamsplitter interaction parameter goes to 0 as the squeezing goes to infinity. This has the following effect on the beamsplitter alone:

$$BS(\theta) = e^{\frac{i\theta}{2}(q_1q_2+p_1p_2)} = \sum_{k=0}^{\infty}\frac{(i\theta)^k}{2^k k!}(q_1q_2+p_1p_2)^k = \mathbb{1} + \frac{i\theta}{2}(q_1q_2+p_1p_2) + \mathcal{O}(\theta^2) \xrightarrow[\theta\to 0]{} \mathbb{1}. \tag{4.33}$$

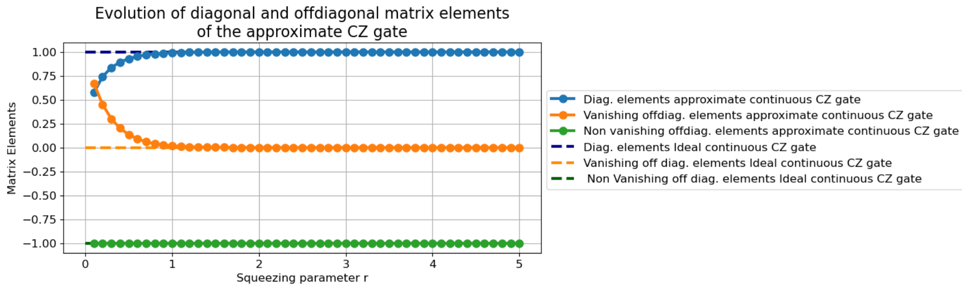

Figure 4.3: Evolution of diagonal and off-diagonal elements of the approximate CZ gate as a function of the squeezing parameter.

This means that once the beamsplitter interaction is sufficiently small it becomes similar to an identity interaction, let us call it $\tilde{\mathbb{1}}$. It follows that numerically the overall effect of the gate is going to be

$$S_2(r)\tilde{\mathbb{1}}S_2(-r) \approx S_2(r)S_2(-r) \approx \mathbb{1}. \tag{4.34}$$

We will see this effect in the analysis that follows.

4.2.1 Numerical analysis of the approximate CZ gate

We first defined a random two qubit input state of the form

$$|\psi_{in}\rangle = |0/1\rangle \otimes (\cos{(\frac{\alpha}{2})}\,|0\rangle + e^{i\beta}\sin{(\frac{\alpha}{2})}\,|1\rangle), \tag{4.35}$$

where α, β are chosen to random numbers between 0 and 1 scaled by 2π and are thus of the form

$$\alpha = \mathrm{rand}(0,1)2\pi, \tag{4.36}$$

and similar for the other parameters. This means that for this part of the simulations we considered non entangled random qubit gates, where we know the state of the control qubit. We then applied the gate, both in its full and its decomposed form, for different squeezings r to the input state. We also defined the the desired output state, which can be analytically calculated and then looked at the various measures introduced before. We also looked at the Bell state $|\Phi^+\rangle$, where some effects of the gate can be observed best, and checks if the same behaviour is also observed for entangled states.
Let us start with the fidelity. In Figure 11 we can see the fidelity of the Bell state with its desired output state after the approximate CZ gate for different squeezings. There are a few things that we can observe:

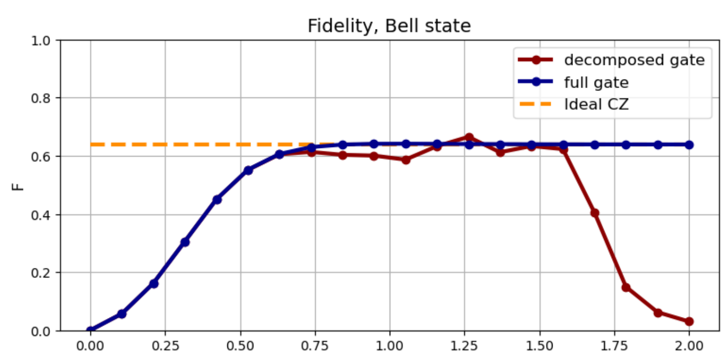

Figure 4.4: Fidelity for the Bell state Φ^+ after the approximate CZ gate for different squeezings. Both the numerical effects in the decomposed version of the gate and the finite energy effects can be observed, as the fidelity does not saturate at 1

First we can see that both the full gate and the decomposed version of the gate converge to the desired ideal value of the CZ gate. This shows that the gate itself converges to the ideal logical CZ gate. We

can furthermore observe the numerical instabilities in the decomposed version of the gate, as after some squeezing the fidelity decays. We observe that for a high enough squeezing, the fidelity even drops to values which are close to 0. This can be explained as in this scenario the decomposed approximate CZ gate is numerically similar to an identity. We therefore compare the only slightly modified Φ^+ state with its orthogonal counterpart Φ^-. There is however one more thing that needs to be observed, namely that the Fidelity only converges to values which are around $F \approx 0.6$ and not to 1, even for the ideal gate. This can also be explained using the results from the ideal gates on finite energy state discussion from before. It follows that even in the best case scenario, where the ideal gate is applied we do not recover the desired output state. We will see later how to overcome this problem using error correction.
Now we can talk about the Holevo phase variance. We will again display the results for the Bell states as it exhibits best the behaviour observed also for random states. Note that we have to consider the Holevo phase variance for both stabilizers, once along q and once along p. In Figure 12 we can see the Holevo phase variance for both stabilizers for the Bell states. The first thing to notice is that we observe

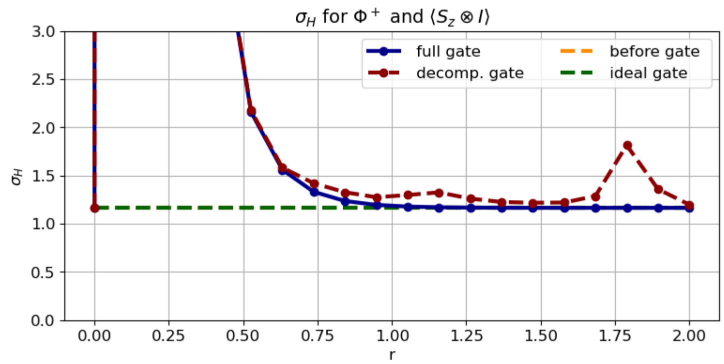

(a) Stabilizer S_z

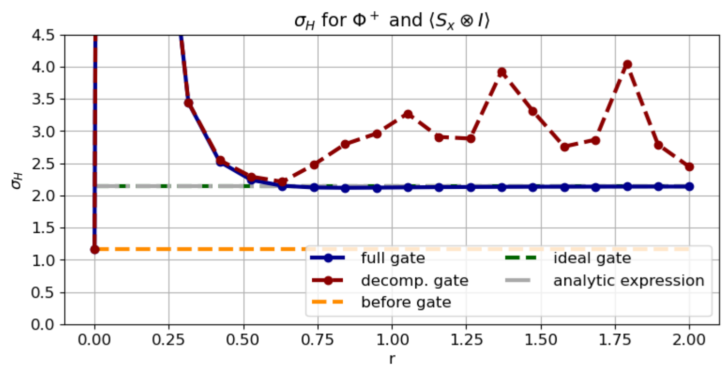

(b) Stabilizer S_x

Figure 4.5: The Holevo Phase variance for the bell state $|\Phi^+\rangle$ as a function of r. We can see that for both stabilizers for sufficiently high squeezing the output state recovers the initial Holevo Phase variance. The ideal CZ gate does not change the Holevo Phase variance.

different behaviours for both stabilizers. First look at the stabilizer S_z. Here both for the full and the decomposed gate we can observe that for small squeezings the state after the gate leave the code space to then return to it if the squeezing is sufficiently strong. For the logical CZ the Holevo phase variance for this state does not change. However this changes as we move to the other stabilizer S_x. Here the Holevo phase variance does not return to its initial value but converges to a larger one. The logical CZ exhibits the same behaviour. Furthermore, we observe strong instabilities in the decomposed version of the gate, which again can be explained by the numerical instabilities of the decomposed approximate CZ gate described before. We can try to understand this offset analytically by calculating the expectation value, which appears in the Holevo phase variance. We will first consider ideal states and then return to finite energy states.
Assume that we start in a perfect $+1$ eigenstate of $S_z \otimes \mathbb{1}$ called $|\psi_1\rangle |\psi_2\rangle$. Then we apply the CZ gate to the initial state and calculate the Holevo phase variance before and after the gate. Before the gate we

obtain:

$$\langle\psi_1|\langle\psi_2| S_z \otimes \mathbb{1} |\psi_1\rangle |\psi_2\rangle = 1, \tag{4.37}$$

since we start in a $+1$ eigenstate of $S_z \otimes \mathbb{1}$. After the gate we obtain:

$$\langle\psi_1|\langle\psi_2| CZ^\dagger (S_z \otimes \mathbb{1}) CZ |\psi_1\rangle |\psi_2\rangle = \langle\psi_1|\langle\psi_2| CZ^\dagger CZ (S_z \otimes \mathbb{1}) |\psi_1\rangle |\psi_2\rangle, \tag{4.38}$$

since CZ and S_z commute. This can then be further simplified, again by using the fact that we are in a $+1$ eigenstate of $S_z \otimes \mathbb{1}$ to

$$\langle\psi_1|\langle\psi_2| CZ^\dagger CZ |\psi_1\rangle |\psi_2\rangle = 1, \tag{4.39}$$

and hence the Holevo phase variance does not change. The same calculation holds for $\mathbb{1} \otimes S_z$. Now we need to consider the other stabilizer $S_x \otimes \mathbb{1}$. We are going to look at an expression looking like this

$$\langle\psi_1|\langle\psi_2| CZ^\dagger (S_x \otimes \mathbb{1}) CZ |\psi_1\rangle |\psi_2\rangle, \tag{4.40}$$

which by means of the Baker-Campbell-Hausdorff formula can be reduced to

$$\langle\psi_1|\langle\psi_2| (S_x \otimes S_z) |\psi_1\rangle |\psi_2\rangle = 1. \tag{4.41}$$

Assuming ideal eigenstates of the stabilizers, the expectation value should be equal to 1. This does not correspond to the observed behaviour.
Therefore we will now assume that the stabilizers only approximately stabilize the code words, such is the case for finite energy GKP states. For simplicity, assume that we want to calculate the expectation value of the stabilizers before and after the gate for the logical $|00\rangle$ state. The expectation value for $S_z \otimes \mathbb{1}$ before the gate is given by

$$\langle 00| S_z \otimes \mathbb{1} |00\rangle \propto e^{-\Delta_1^2 \pi} \sum_{s_1,s_2,s_3,s_4} e^{-\frac{\kappa_1^2}{2}(2s_1\sqrt{\pi})^2} e^{-\frac{\kappa_2^2}{2}(2s_2\sqrt{\pi})^2} e^{-\kappa_1^2 2(2s_3\sqrt{\pi})^2} e^{-\frac{\kappa_2^2}{2}(2s_4\sqrt{\pi})^2} e^{-\frac{\pi(s_1-s_3)^2}{\Delta_1^2}} e^{-\frac{\pi(s_2-s_4)^2}{\Delta_2^2}}. \tag{4.42}$$

This expression does not change after the gate, since as we have seen CZ and S_z commute. This is in accordance with the observed result. For the other stabilizer we can again first look at what we have before the gate:

$$\langle 00| S_x \otimes \mathbb{1} |00\rangle \propto \sum_{s_1,s_2,s_3,s_4} e^{-\frac{\kappa_1^2}{2}(2s_1\sqrt{\pi})^2} e^{-\frac{\kappa_1^2}{2}(2s_3\sqrt{\pi})^2} e^{-\frac{\kappa_2^2}{2}(2s_2\sqrt{\pi})^2} e^{-\frac{\kappa_2^2}{2}(2s_4\sqrt{\pi})^2} e^{-\frac{\pi(s_1-s_3)^2}{\Delta_1^2}} e^{-\frac{\pi(s_2-s_4)^2}{\Delta_2^2}} \tag{4.43}$$

After the gate however we have seen how the expectation value transforms in equation (4.41). Using this result, and the results from equation (4.43) and (4.42) we obtain

$$\langle 00| S_x \otimes S_z |00\rangle \propto e^{-\Delta_2^2 \pi} \langle 00| S_x \otimes \mathbb{1} |00\rangle. \tag{4.44}$$

The appearing prefactor reduces the expectation value, hence increases the Holevo phase variance. The Holevo phase variance after the gate for the stabilizer $S_x \otimes I$ can thus be written as

$$\sigma_{H,CZ} = e^{\Delta_2^2 \pi} \sqrt{|\langle 00|S_x \otimes I|00\rangle|^{-2} - e^{-2\Delta_2^2 \pi}}. \tag{4.45}$$

This is the effect we see in Figure 12b. We can now look at the effective squeezing parameters. Here we can observe again that the behaviour of the parameters change depending on the stabilizer that we look at. This is once again expected, as both the Holevo phase variance and the effective squeezing parameters contain the same physical quantities. We can see this behaviour in Figure 13.

We can see a change in the width of the peaks in p space after the CZ (or the approximate CZ) gate. We can quantify this behaviour using the results from the Holevo phase variance from before. Assume we are looking at the change in p-space on the control qubit. Consider the $|00\rangle$ state as an input. Then we can write the change as:

$$\Delta'_{p_1} \propto \sqrt{\frac{1}{2\pi} \ln\left(\frac{1}{|\langle 00| S_x \otimes S_z |00\rangle|^2}\right)} = \sqrt{\Delta_{q_2}^2 + \Delta_{p_1}^2} \tag{4.46}$$

We have seen before the effects of the approximate and the ideal CZ gate on a finite energy state are non trivial. We extend this discussion now to the CNOT.

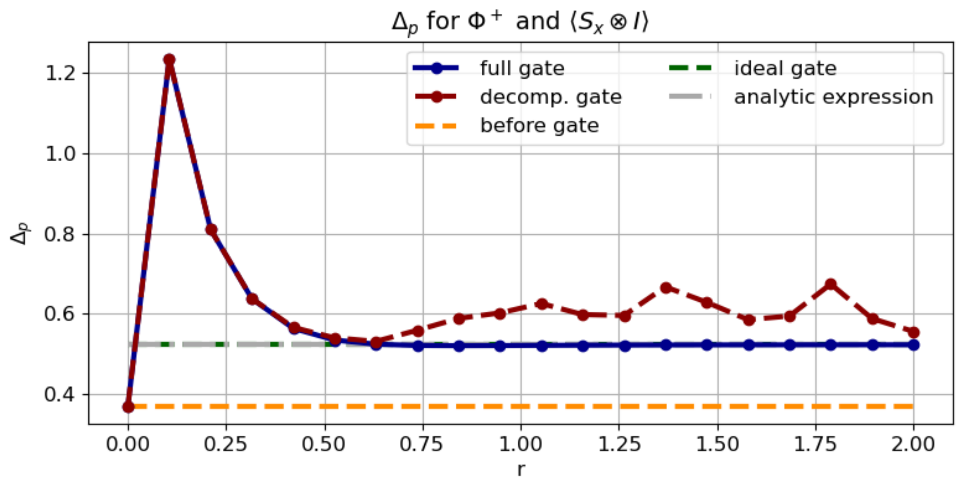

Figure 4.6: The effective squeezing parameters for $\langle S_x \otimes I \rangle$. We can observe a similar behaviour to what we have already seen in the Holevo Phase variance.

4.3 The CNOT decomposition

In this section we are going to analyse the proposal for a logical CNOT from the work of Tzitrin et al. [25], which uses the Bloch Messiah decomposition as described before. Other proposals, such as in Terhal et al.[24], are not going to be considered here. This gate is, if implemented properly, exact and not an approximation. It consists of a beamsplitter followed by a squeezer and a beamsplitter with a different angle. This can be seen in Figure 14. Tzitrin et al. use the alternate description of the beamsplitter

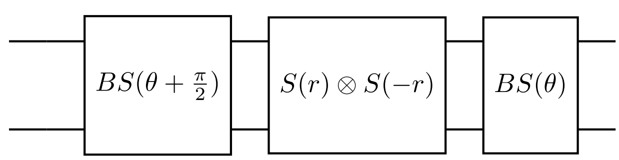

Figure 4.7: Decomposition of the CNOT gate. This gate uses the Bloch-Messiah decomposition and is therefore exact.

given in equation (4.14). The starting point for this gate is a generalized CNOT, which is the SUM gate and is given by

$$\mathrm{SUM}(g) = e^{-igq_1p_2}. \tag{4.47}$$

The SUM gate implements a CNOT if $g = (2k+1), k \in \mathbb{Z}$. The decomposition above implements this gate if the following conditions hold:

$$\sin(2\theta) = -\mathrm{sech}(r) \tag{4.48}$$
$$\cos(2\theta) = \tanh(r) \tag{4.49}$$
$$\sinh(r) = -\frac{g}{2}. \tag{4.50}$$

While in the paper the authors state that the standard weight is $g = 1$, we will use the weight $g = -1$ to avoid negative squeezing in the simulations. From the conditions stated in equation (4.48) we can find the following relation between the angle and the squeezing strength:

$$\theta(r) = \frac{1}{2}\arctan\Big(-\frac{1}{\sinh(r)}\Big) \tag{4.51}$$

The behaviour of this parameter can be seen in Figure 15. In Figure 16 we can see the allowed values for the squeezing in order to implement a CNOT

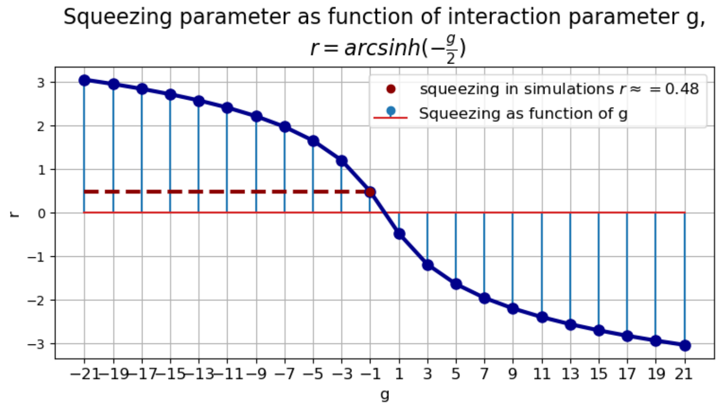

Figure 4.8: The squeezing parameter as a function of the interaction parameter g for the decomposition of the CNOT gate. The red dot indicates the value corresponding to the ideal CNOT gate in our simulations

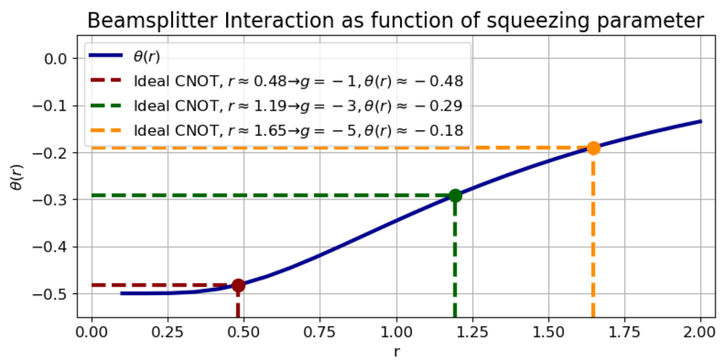

Figure 4.9: Beamsplitter interaction for the decomposed CNOT gate. The values, where the ideal CNOT occurs are indicated.

As a quality measure we are only looking at the fidelity for this specific gate, for a more thorough analysis please refer to the original paper . We are using as an input state the state $|{+0}\rangle$, since this state under application of the CNOT should result in a maximally entangled state Φ^+. Furthermore, Tzitrin et al. use this input state as well for their simulations in their paper. We simulated the decomposition of the CNOT gate for different squeezings, not only the squeezings in order to implement an ideal CNOT. The results of the fidelity of the state $\text{CNOT}_{decomp}(r, \theta)\,|{+0}\rangle$ with its ideal output state Φ^+ is given in Figure 17. We can see that we again do not reach ideal fidelity, even for the ideal CNOT gate, which

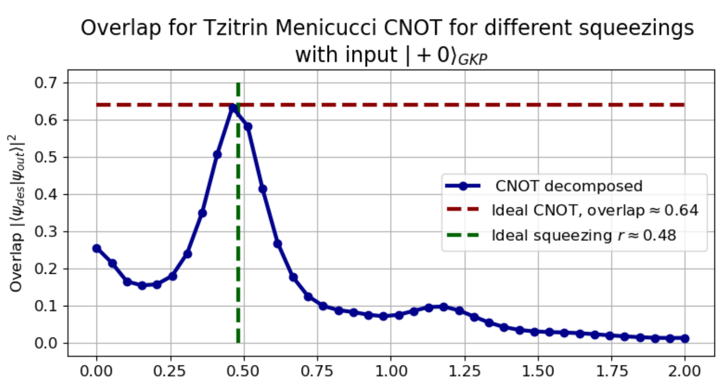

Figure 4.10: Fidelity simulations of the decomposed CNOT gate. We can see that at $r \approx 0.48$ the ideal gate occurs. We can again observe finite energy effects due to not reaching an ideal fidelity of 1.

means that we again have to take into account finite energy effects. Furthermore we can observe that for $r \approx 0.48$ we obtain the Ideal CNOT with our simulations. It becomes also evident that this gate, in order to work properly, has to be calibrated very precisely. Slight deviations from the ideal squeezing result in a decay away from the ideal value. We can observe another peak at approximately 1.16 which is again a peak where an ideal CNOT occurs. It is not surprising that the finite energy effects reduce the fidelity similarly to the approximate and ideal CZ gate, since the CNOT and the CZ are linked via a Fourier transform on the target qubit. From this plot we can see that, while the decomposition of the CNOT implements an ideal CNOT under specific circumstances, it seems to be more sensible in the deviation of the squeezing, compared to the approximate CZ gate. The approximate CZ gate, once a specific squeezing r_{th} is surpassed, implements for all $r > r_{th}$ approximately the same gate.
To further compare the two different approaches, we can compare the behaviour of the beamsplitter parameters for both gates and its derivatives. This can be seen in Figure 18. We can observe that the

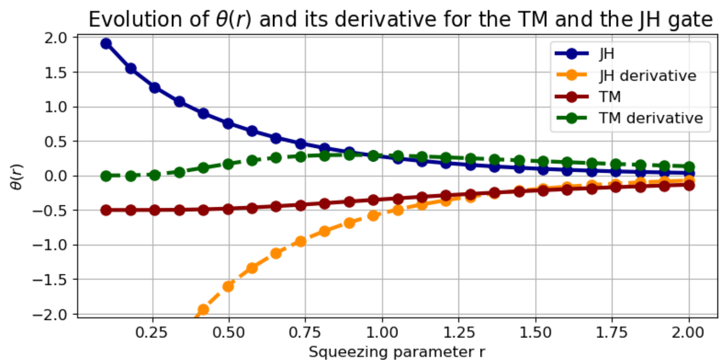

Figure 4.11: Comparison of the different beamsplitter parameters.

derivative of the beamsplitter parameter of the approximate CZ gate diverges as $r \to 0$. This could insinuate that for small squeezings the implementation of this gate might be unstable. However as we have seen for small squeezings the approximate CZ gate does not implement a CZ and therefore this behaviour can be discarded. We have to consider however that for large squeezings the approximate CZ exhibits numerical instabilities. This could suggest that only a small range of squeezings could be used in an experimental setting, if the numerical instabilities translate into physical ones. Experimental results would be necessary to test this result.
The decomposed CNOT on the other hand does not exhibit divergences in its beamsplitter parameter. However as we have seen in the plots for the fidelity the relevant parameters have to calibrated with much more caution in order to obtain the desired fidelity outcome.

Chapter 5

Quantum error correction for logical GKP gates

We have seen that ideal GKP gates produces errors in finite energy GKP states. We have observed a reduction in the amplitude and a broadening of the envelope in the discussion of the change of the wave function under application of the logical CZ. We will now look if we can correct for said errors using quantum error correction. We will use the error correction approach by De Neeve et al. [17] and then look how this correction scheme performs for our gates. While the main purpose of this thesis is not to exhibit the strength of quantum error correction schemes, this section is designed to show that the errors from the CZ gate can be corrected.

5.0.1 Error correction scheme using dissipative pumping

We will describe here a single round of error correction using the scheme described in [17]. During this process we will couple our GKP state to an ancilla spin. To distinguish the operators acting on the spin and the operators acting on our CV mode we will introduce the following notation: A logical Pauli X operator acting on the spin is going to be represented by the Greek letter σ_x, whereas an operator on the continuous variable mode is going to be represented as before using the capital letter X. Each round of correction corresponds to an application of two different unitaries, in order to account for the correction both in position and in the momentum quadrature. The two unitaries are given by

$$U_1 = e^{i\mu p\sigma_y} e^{i\alpha q\sigma_x} e^{i\epsilon p\sigma_y} \qquad \text{and} \qquad U_2 = e^{i\mu q\sigma_y} e^{-i\alpha p\sigma_x} e^{i\epsilon q\sigma_y}. \tag{5.1}$$

The parameters have been optimized to maintain an envelope and a single peak width of $\Delta = \kappa = 0.37$ and are given by

$$\alpha = \sqrt{\pi}, \qquad \mu = 2\sqrt{\pi}0.065 \qquad \text{and} \qquad \epsilon = 2\sqrt{\pi}0.045 \tag{5.2}$$

Once the cycle is over, we can perform a partial trace over the ancilla spin and compare the corrected state to the desired state. Various other methods such as the BigSmallBig and the SmallBigSmall and the methods are described in Royer et al. [21] are not considered for this discussion here. While the correction operators are unitary, the error correction process is not. The tracing out after every round of error correction dissipates the detected errors.

5.0.2 Correction Protocol

For this section assume that a random two qubit state has to pass a logical CZ gate. For the algorithm we will assume the following routine:

1. We apply the stabilization routine to our input state and to our desired output state. Then we will calculate the fidelity with the desired ideal finite energy state for both modes. This allows us to get an intuition on how good the fidelity can get in the stabilization process. The stabilization of the input state ensures that the error correction protocol does not bias the output.

2. We apply the CZ gate to our stabilized input. We then calculate the fidelity of the output with the ideal finite energy state.

3. We stabilize the output and calculate the fidelity measure again to see how good the stabilization process made our state return to the desired output state.

In Figure 19 a) we can see the fidelity of the input state with the desired input state as a function of the stabilization cycles. We can observe a drop of the fidelity in the beginning and a saturation at around $F \approx 0.7$ after 6 stabilization rounds. The fidelity drop can be explained since in the stabilization process we are trying to correct our state to a state with a different envelope, since the parameters are optimized for states with an envelope of $\kappa = 0.37$. In Figure 19 b) we can see the fidelity for the stabilization of the desired output state. The observed behaviour is very similar.

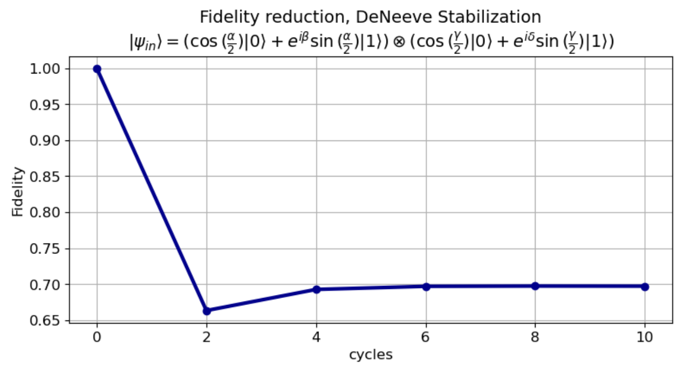

(a) Stabilization of the desired input state.

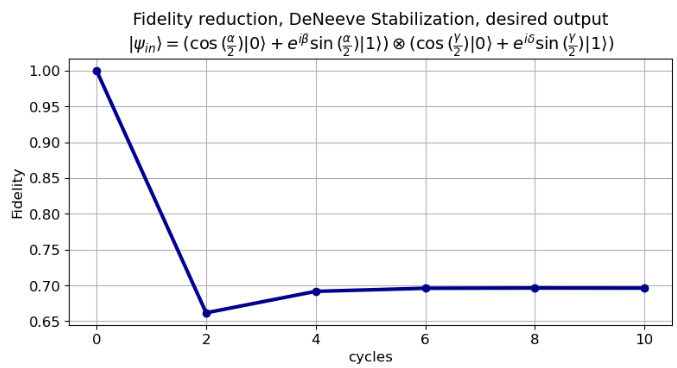

(b) Stabilization of the desired output state.

Figure 5.1: Stabilization of the input and the output state. A drop of fidelity is observed towards the first rounds of stabilization and saturation occurs after ca. 6 rounds.

We chose the state after 6 stabilization rounds for our input state. Following the protocol explained above we stabilize the output. The fidelity increase of this process is given in figure 20. We can see from this plot that the state after stabilization returns to the optimal fidelity with the desired state. We can however observe that not a perfect fidelity is reached. Other stabilization processes might bring an improvement to this.
Concluding we find that in order to obtain a working logical CZ gate in a finite energy GKP qubit setting it is necessary to both have the tools to implement the gate and to correct for the error.

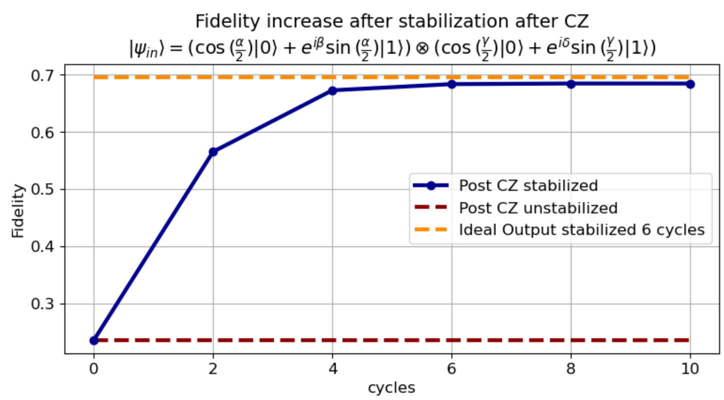

Figure 5.2: Stabilization of the output state. We can see that the stabilization process increases the fidelity, and after ca. 6 rounds the fidelity with the desired output state is reached.

Chapter 6

Conclusion & Outlook

In this thesis we have looked at finite energy effects of an ideal GKP CZ and CNOT gate on a finite energy two qubit state. We have seen that non trivial effects can be observed in the p quadrature of phase space and we have seen how to quantify the induced error to some extent. A full description of the induced error would allow to construct error correction schemes precisely.

We have furthermore looked into a new implementation of the CZ gate using linear optical elements, which as opposed to already existing schemes shows less sensitivity to a non perfect calibration of the squeezing parameter after a specific threshold is surpassed.

We have seen that the errors induced by the gate, although not fully described, can be corrected using existing error correction schemes using dissipative pumping. However the correction is not perfect, due to being optimized to parameters different from the ones used in our simulations. Due to time issues we could not investigate other error correction schemes, that might produce better results in the fidelity.

There are however still some unanswered questions. One question concerns the resources needed to be able to implement a circuit using multiple two qubit CZ gates. Consider for example a graph state, as used in Measurement Based Quantum Computation. Here physical qubits are entangled to their nearest neighbours using CZ gates. It seems from our analysis however that for each physical qubit in the state preparation we need multiple rounds of correction. It would be interesting to quantify this in terms of resources and ancillas needed.

Another interesting research area would be the realization of a finite energy version of the gate, as briefly described in the very beginning of this thesis. Although requiring non unitary operations this would give a great insight into the connection between ideal and finite energy GKP states.

This thesis both underlined the strengths and the weaknesses of GKP Qubits. One strength is that they use harmonic oscillators as their resource. Harmonic oscillators are the main interest in both photonic and trapped ion systems and are therefore experimentally accessible. Another strength is the elegance of the ideal GKP code, since it translates the concepts of discrete variable quantum computation into continuous variable systems by exploiting a translational symmetry of the system. The biggest downside in my opinion is that the ideal code is not realizable in a physical system. The realizable code is only an approximation and as we have seen, there are additional resources required to take into account the errors created by these imperfections.

Bibliography

[1] Frank Arute et al. “Quantum supremacy using a programmable superconducting processor”. In: *Nature* 574.7779 (2019), pp. 505–510. DOI: https://doi.org/10.1038/s41586-019-1666-5.

[2] Stephen D. Bartlett et al. “Efficient Classical Simulation of Continuous Variable Quantum Information Processes”. In: *Physical Review Letters* 88.9 (2002). DOI: 10.1103/physrevlett.88.097904. URL: https://doi.org/10.1103%2Fphysrevlett.88.097904.

[3] G. Blaizot J.-P.; Ripka. “Quantum Theory of Finite Systems”. In: *MIT Press* (1985).

[4] N.N Bogoljubov. “On a new method in the theory of superconductivity”. In: *Nuovo Cim.* 7 (1958). DOI: https://doi.org/10.1007/BF02745585.

[5] J. Eli Bourassa et al. “Fast Simulation of Bosonic Qubits via Gaussian Functions in Phase Space”. In: *PRX Quantum* 2 (4 2021), p. 040315. DOI: 10.1103/PRXQuantum.2.040315. URL: https://link.aps.org/doi/10.1103/PRXQuantum.2.040315.

[6] Samuel L. Braunstein. “Squeezing as an irreducible resource”. In: *Phys. Rev. A* 71 (5 2005), p. 055801. DOI: 10.1103/PhysRevA.71.055801. URL: https://link.aps.org/doi/10.1103/PhysRevA.71.055801.

[7] Deutsch David. “Quantum theory, the Church–Turing principle and the universal quantum computer”. In: *Proc. R. Soc. Lond.* A40097–117 (1985). DOI: http://doi.org/10.1098/rspa.1985.0070.

[8] Weigand D.J. *Encoding a Qubit into an Oscillator with Near-Term Experimental Devices*. 2020. DOI: https://doi.org/10.4233/uuid:72abf99f-dd2d-42a1-8c59-7a83870c9d3c.

[9] Daniel Gottesman. “Stabilizer Codes and Quantum Error Correction”. In: (1997). DOI: 10.48550/ARXIV.QUANT-PH/9705052. URL: https://arxiv.org/abs/quant-ph/9705052.

[10] Daniel Gottesman. “Theory of fault-tolerant quantum computation”. In: *Physical Review A* 57.1 (1998), pp. 127–137. DOI: 10.1103/physreva.57.127. URL: https://doi.org/10.1103%2Fphysreva.57.127.

[11] Daniel Gottesman, Alexei Kitaev, and John Preskill. “Encoding a qubit in an oscillator”. In: *Physical Review A* 64.1 (2001). DOI: 10.1103/physreva.64.012310. URL: https://doi.org/10.1103%2Fphysreva.64.012310.

[12] Lov K. Grover. *A fast quantum mechanical algorithm for database search*. 1996. DOI: 10.48550/ARXIV.QUANT-PH/9605043. URL: https://arxiv.org/abs/quant-ph/9605043.

[13] Sebastian Krämer et al. “QuantumOptics. jl: A Julia framework for simulating open quantum systems”. In: *Computer Physics Communications* 227 (2018), pp. 109–116.

[14] Seth Lloyd and Samuel L. Braunstein. “Quantum Computation over Continuous Variables”. In: *Physical Review Letters* 82.8 (1999), pp. 1784–1787. DOI: 10.1103/physrevlett.82.1784. URL: https://doi.org/10.1103%2Fphysrevlett.82.1784.

[15] Takaya Matsuura, Hayata Yamasaki, and Masato Koashi. “Equivalence of approximate Gottesman-Kitaev-Preskill codes”. In: *Phys. Rev. A* 102 (3 2020), p. 032408. DOI: 10.1103/PhysRevA.102.032408. URL: https://link.aps.org/doi/10.1103/PhysRevA.102.032408.

[16] Lucas J. Mensen, Ben Q. Baragiola, and Nicolas C. Menicucci. “Phase-space methods for representing, manipulating, and correcting Gottesman-Kitaev-Preskill qubits”. In: *Phys. Rev. A* 104 (2 2021), p. 022408. DOI: 10.1103/PhysRevA.104.022408. URL: https://link.aps.org/doi/10.1103/PhysRevA.104.022408.

[17] Brennan de Neeve et al. "Error correction of a logical grid state qubit by dissipative pumping". en. In: *Nature Physics* (Feb. 2022). Publisher: Nature Publishing Group, pp. 1–5. ISSN: 1745-2481. DOI: 10.1038/s41567-021-01487-7. URL: https://www.nature.com/articles/s41567-021-01487-7 (visited on 02/09/2022).

[18] Michael A. Nielsen and Isaac L. Chuang. *Quantum Computation and Quantum Information: 10th Anniversary Edition*. Cambridge University Press, 2010. DOI: 10.1017/CBO9780511976667.

[19] A M Perelomov. "Generalized coherent states and some of their applications". In: *Soviet Physics Uspekhi* 20.9 (1977), pp. 703–720. DOI: 10.1070/pu1977v020n09abeh005459. URL: https://doi.org/10.1070/pu1977v020n09abeh005459.

[20] Ivan Rojkov. "CVsim.jl: Continuous Variables simulations in Julia". In: *Gitlab, private repository* (2022).

[21] Baptiste Royer, Shraddha Singh, and S. M. Girvin. "Stabilization of Finite-Energy Gottesman-Kitaev-Preskill States". In: *Phys. Rev. Lett.* 125 (26 2020), p. 260509. DOI: 10.1103/PhysRevLett.125.260509. URL: https://link.aps.org/doi/10.1103/PhysRevLett.125.260509.

[22] Peter W. Shor. "Polynomial-Time Algorithms for Prime Factorization and Discrete Logarithms on a Quantum Computer". In: *SIAM Journal on Computing* 26.5 (1997), pp. 1484–1509. DOI: 10.1137/s0097539795293172. URL: https://doi.org/10.1137%2Fs0097539795293172.

[23] Peter W. Shor. "Scheme for reducing decoherence in quantum computer memory". In: *Phys. Rev. A* 52 (4 1995), R2493–R2496. DOI: 10.1103/PhysRevA.52.R2493. URL: https://link.aps.org/doi/10.1103/PhysRevA.52.R2493.

[24] B M Terhal, J Conrad, and C Vuillot. "Towards scalable bosonic quantum error correction". In: *Quantum Science and Technology* 5.4 (2020), p. 043001. DOI: 10.1088/2058-9565/ab98a5. URL: https://doi.org/10.1088/2058-9565/ab98a5.

[25] Ilan Tzitrin et al. "Progress towards practical qubit computation using approximate Gottesman-Kitaev-Preskill codes". In: *Phys. Rev. A* 101 (3 2020), p. 032315. DOI: 10.1103/PhysRevA.101.032315. URL: https://link.aps.org/doi/10.1103/PhysRevA.101.032315.

[26] Christian Weedbrook et al. "Gaussian quantum information". In: *Reviews of Modern Physics* 84.2 (2012), pp. 621–669. DOI: 10.1103/revmodphys.84.621. URL: https://doi.org/10.1103%2Frevmodphys.84.621.